VOLUME 19, 1957/58, No. 12 pp. 333-364 Published 22nd August 1958

Philips Technical Review

DEALING WITH TECHNICAL PROBLEMS
RELATING TO THE PRODUCTS, PROCESSES AND INVESTIGATIONS OF
THE PHILIPS INDUSTRIES

THE DOUBLE-FLUX "TL" LAMP, A FLUORESCENT LAMP OF HIGH OUTPUT PER UNIT LENGTH

by H. J. J. van BOORT and D. KOLKMAN. 621.327.534.15

A minor modification in the design of Philips tubular fluorescent lamps has made it possible to attain, with a satisfactory efficiency, about double the luminous flux normally obtained in fluorescent lamps of the same length. For a variety of purposes, such as the lighting of factory workshops, sports halls, etc., these new lamps will make possible more economical installations.

Although the fields of application of incandescent lamps and tubular fluorescent lamps ("TL" lamps) are now fairly clearly defined — they enjoy a sort of peaceful co-existence — we are reminded from time to time of some valuable properties of the incandescent lamp that are missing in the fluorescent lamp. One of these properties is the concentration of a large output in a relatively small and easily manipulated lamp. Incandescent lamps up to 1500 W are still classed as "ordinary" lamps, i.e. as lamps requiring no special methods and procedures in manufacture or in handling (for connection, maintenance and replacement). Far larger incandescent lamps, up to 10 kW or even more, are regularly manufactured and even these can be reasonably manipulated. The world success of the fluorescent lamp, on the other hand, has been achieved largely with a single version, viz. that with an output of approx. 40 W and a length of about 1.20 m. Until recently it seemed that a substantially larger power could not be obtained in a lamp of this length without largely sacrificing the advantage of its high luminous efficiency.

This restriction in power was an unsatisfactory state of affairs. For high light level industrial and street-lighting installations, for which fluorescent light is so eminently suitable as regards colour and efficiency, it is most desirable that the luminous flux of each lamp be as high as possible: fewer lamps are then required, costs of fixtures and ballasts are thereby lowered and maintenance is cheaper. The rather trivial measure of making the lamps longer whilst retaining about the same power per unit length, however, is not a real solution at all. The fixtures may be fewer in number, but will also be more expensive, and the same applies to the ballasts, owing to the ignition voltage increasing with the length of the lamp. Apart from that comes the fact that replacing very long lamps, for instance 125 W lamps with a length of 2.40 m, in an installation for industrial or street lighting is no easy matter.

Lamp manufacturers have now succeeded, in various ways, in developing fluorescent lamps with a larger output, whilst retaining a reasonable length and a high luminous efficiency. In order to appreciate the modifications introduced for this purpose, let us first examine the factors determining the efficiency of the fluorescent lamp.

Efficiency and dimensions of tubular fluorescent lamps

The basic process in lamps of this type is the emission of ultraviolet radiation quanta, mainly at a wavelength of 2537 Å, by mercury atoms in an excited state, and the absorption of these quanta by the fluorescent powder deposited on the tube wall. The larger the number of mercury atoms present, i.e. the higher the mercury-vapour pressure in the tube and the larger the current density of the electric discharge, the more mercury atoms will be excited by the electrons accelerated in the electric field (the primary process). At the same time, however, two secondary phenomena which impair efficiency become increasingly manifest: these are self-absorption, i.e. the absorption of radiation quanta by unexcited mercury atoms, and the raising of excited mercury atoms to higher energy levels. In either case, it is true, a 2537 Å radiation quantum may be re-emitted, but the competing processes, namely the emission of quanta of larger or smaller wavelength, which are unsuitable for producing fluorescence, and the dissipation of excitation energy in the form of heat, are favoured by these intermediate excitation stages [1]). Particularly adverse is the effect of a rise in mercury-vapour pressure. On the other hand, some mercury pressure is obviously essential to the primary process. An optimum light efficiency is found at a specific mercury-vapour pressure, viz. at approx. 5×10^{-3} mm Hg. This corresponds to the saturation vapour pressure of mercury at a temperature of about 40 °C.

"TL" lamps (being provided with a small surplus of liquid mercury) are accordingly always made in such a way that the tube wall will assume a temperature of about 40 °C when the lamp is burning under ordinary conditions. It is the wall of the tube, being the coldest part of the lamp, which determines the equilibrium pressure of the mercury vapour. In ordinary "TL" lamps the tube wall assumes this temperature along nearly the whole discharge column; near the electrode it is generally warmer.

Once the wall temperature of the discharge column is specified, a certain relationship will hold between the power to be developed in the discharge column and the dimensions of the tubular lamp: for a given ambient temperature, generally taken as 25 °C [2]), and for a given wall temperature, the amount of heat q dissipated per unit time from each unit area of the wall by radiation and convection, may be considered as a fixed value. In actual fact, this amount q depends to some degree upon the diameter d of the tube (q decreases as d is made larger), but this may be disregarded to a first approximation. Consequently, if the discharge column is to handle a power P, a wall area $A = P/q$ is required.

Let us now assume that we wish to double the power developed in the column. This means that also the wall area has to be approximately doubled. One obvious way to do so is as already mentioned, viz. by making the column twice as long with the same diameter. This has more or less the same effect as if two of the original lamps were placed end to end. We have already mentioned that this is no adequate solution: the lamp becomes undesirably long and also the voltage V_z across the column becomes far too high, viz. twice the original value. An effective lamp design is one for which the burning voltage (i.e. arc voltage V_z + the voltage loss at the electrodes, the latter being about 15 V for "TL" lamps) is approximately half the r.m.s. value of the mains voltage (or, more accurately: of the open voltage of the ballast). A higher burning voltage is not favoured, because then the lamp would be unduly affected by mains-voltage fluctuations. This could be compensated by stepping-up the mains voltage, but that would again lead to a more expensive ballast.

Another method of obtaining double the wall area would be to double the diameter whilst retaining the original length of the column. This would be a good solution, where easy handling of the lamp is concerned, but the overall efficiency would be very poor. With such a diameter the arc voltages become very low, whilst the current becomes very large (the arc-discharge gradient decreases with increasing diameter and with increasing current, see below). For a very low arc voltage the contribution of the constant voltage loss of 15 V at the electrodes would impair the total efficiency to such an extent that it would more than offset the advantage of having maintained the correct wall temperature and accordingly the optimum mercury-vapour pressure. The large current and low voltage, moreover, would again require a relatively expensive ballast.

An obvious compromise between these two extreme possibilities (constant diameter d or constant length l) would be to double the wall area $A = \pi dl$ whilst retaining the burning voltage. Both length and diameter must then be greater than those of the original lamp. The required values can be approximately found with the aid of a graph giving the experimentally determined gradient of the low-pressure mercury discharge as a function of the diameter, for various values of the current; see *fig. 1*. The procedure is explained in the caption to the graph. The result is a roughly geometrically-similar enlargement of the original lamp: both length and diameter have to be enlarged by a factor of about $\sqrt{2}$ to double the power; see *fig. 2*.

This may be illustrated by the following numerical example. The well-known "TL" 65 W lamp, which has been manufactured for some years now, has a burning voltage of 110 V and hence a voltage $V_z = 110 - 15 = 95$ V across the column; the power developed in the column is approximately 55 W. The internal diameter of the lamp is 35 mm and its length about 1.50 m; for the electrode spaces and the transition zones between column and electrode about 10 cm should be allowed, so that the column has a length of approx. 1.40 m. Doubling the power developed in the column to 110 W, according to fig. 1, would lead to a lamp having a column length of approx. 2.20 m and an internal diameter of 48 mm.

---

[1]) See e.g. G. Heller, Comparison between discharge phenomena in sodium and mercury vapour lamps, Philips tech. Rev. 1, 2-5 and 70-75, 1936.

[2]) In accordance with the international agreement to measure the luminous flux and hence also the luminous efficiency of fluorescent lamps always at an ambient temperature of 25 °C.

The foregoing evidently does not reveal what the consequences are if we depart from the prescribed relation between l and d, i.e. to what extent the luminous efficiency of the lamp would be impaired if the wall temperature were allowed to assume a value different from the optimum 40 °C. A quantitative evaluation of this effect would exceed the scope of this article, the more so since we have to consider that this efficiency does not depend on the mercury pressure alone. The influence of the current density we have mentioned earlier; additional factors are the pressure of the rare gas present to aid in the ignition of the lamp, the length of the free path of the radiation quanta from the interior of the column to the wall, the recombination of ions and electrons at the wall, etc. The simplest way of demonstrating the importance of the correct wall temperature, that is to say, of the correct specific loading, is to carry out an experiment. For this purpose we have measured the luminous efficiency of a given ordinary "TL" lamp as a function of the load; see *fig. 3*. We then find that by increasing the power to double the rated value, the luminous flux is raised by only 40%. The luminous efficiency of the lamp has therefore dropped by 30%. A noticeable reduction in luminous efficiency (viz. by 5%) is even apparent when the rated power is exceeded by as little as 16%.

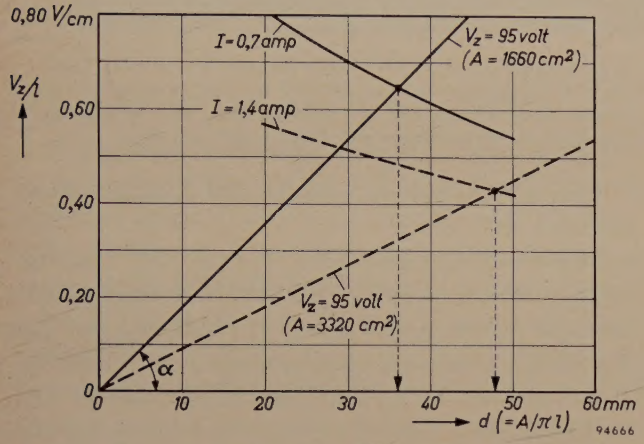

Fig. 1. The curved lines show how the gradient V_z/l in the column of a low-pressure mercury discharge varies as a function of the internal diameter d, for various discharge currents I (for an argon pressure of 1.5 mm Hg).

Given a certain wall temperature, then for a prescribed power P developed in the column, the wall area A may be considered roughly as fixed; hence the abscissa scale for d $(= A/\pi l)$ at the same time represents a reciprocal scale of the column length l. On any straight line through the origin, therefore, the voltage V_z has a constant value, and the required value of d (and hence of l) for given values of P and V_z is given by the intersection of the curve corresponding to the current I with the straight line appropriate to V_z.

For a larger current, corresponding to a larger power P (and therefore larger A), the V_z/l curve lies lower (dotted curve); also the slope of the straight line for the same value of V_z is less. (The slope of this straight line is tan $\alpha = \pi V_z/A$, and is therefore, at constant V_z, smaller for the larger area A corresponding to the higher value of P.) The new point of intersection occurs at a larger diameter and length, these being roughly proportional to the square root of the power.

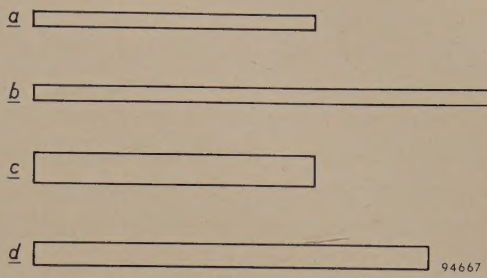

Fig. 2. Given a tubular fluorescent lamp of a certain power, a lamp with double the power may be realized in various ways:
a) Original lamp.
b) Lamp with the same diameter and double the length; the arc voltage is doubled.
c) Lamp having the same length as (*a*) but with double the diameter; the arc voltage becomes very low.
d) Lamp having the same arc voltage as (*a*); both length and diameter have been increased; the proportions of the lamp are similar to (*a*).

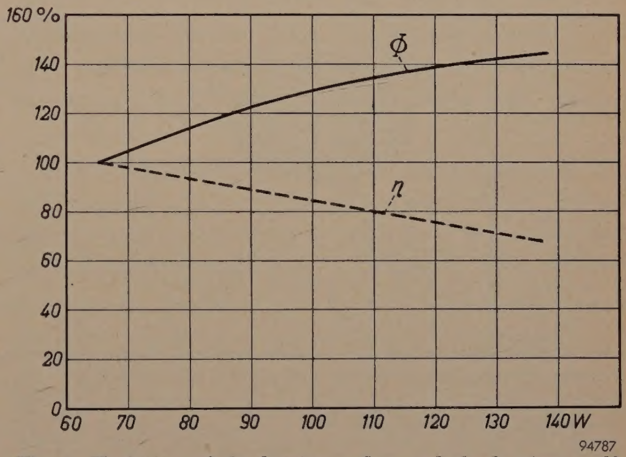

Fig. 3. Variation of the luminous flux and the luminous efficiency (both plotted as percentages of the rated values) of a given "TL" 65 W lamp for various values of the power developed in it. The lamp was not of course operated with its ordinary ballast: it was fed from a special supply. (The lamp differed from the ordinary "TL" 65 W lamps only in having somewhat heavier electrodes, fitted for the purpose of this experiment to withstand the larger current.)

Fluorescent lamps for increased power per unit length

The foregoing considerations led to the conclusion that for a larger power a longer fluorescent lamp would be necessary. On further consideration, however, we find that this is due to the implicit assumption that the temperature determining the mercury-vapour pressure in the tube (the temperature of the coldest spot of the tube) should be the same as that determining the amount of heat carried off per cm² of the wall (some form of average wall temperature). This provides the clue showing the direction one must take in order to develop a larger power in a fluorescent lamp without appreciably increasing its length: the design of the lamp should be changed such that, *with a higher average wall temperature, there remains at least one spot where the temperature of the wall is about 40 °C.*

We shall now discuss three designs of fluorescent lamps in which this principle has been employed: the "Power Groove" lamps of General Electric, U.S.A., the "V.H.O." (very high output) lamps of Sylvania, and the "TL" double-flux lamps developed by Philips.

The design of the "Power Groove" lamps [3]) is based on a tube with a diameter of 53 mm, the cross-section of which has been deformed into the kidney-shape shown in *fig. 4.* Since a groove running over the entire length of the lamp would reduce the mechanical strength, thus increasing the risk of implosion, the lamp has been allowed to retain some lengths of circular cross-section at the ends and at a few regular intervals in between. The discharge mainly concentrates in the shaded part of the cross-section. The lower parts of the cross section (the lamp is mounted in the position shown in fig. 4) remain relatively cool. Having a length of 1.20 m, such a lamp can be loaded with 107 W (current 1.5 A at a voltage of 84 V) and then has a luminous efficiency of 56 lm/W, measured after 100 burning hours.

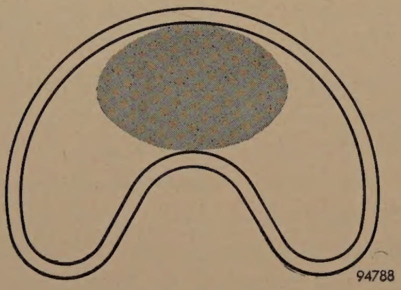

Fig. 4. Cross-section of the "Power-Groove" lamp (General Electric [3])). The discharge is more or less concentrated in the shaded part; in the lower points of the cross-section the wall remains at a lower temperature.

The "V.H.O." lamps [4]) have a normal circular cross-section with a diameter of 38 mm, but for their given total length of 1.20 m the distance between the electrodes is smaller than normal. Thus, behind each electrode remains a space with a length of about 6 cm in which no discharge takes place (*fig. 5*). This space is moreover screened off from the radiant heat of the electrode by a metal plate, and is thus more or less separated from the discharge section. This makes it possible to keep the wall temperature at the end of the tube at about 40 °C, with a load of 100 W. Neon is used as the ignition gas instead of the customary argon.

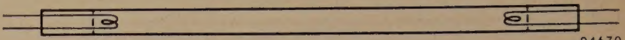

Fig. 5. Sketch of the "Very High Output" lamps (Sylvania [4])). Here the sections situated behind the electrodes, which are longer than normal and screened off from the heat radiated by the electrodes, remain at a temperature of 40 °C.

Current and burning voltage of this lamp amount to 1.2 A and 99 V.

The Philips-designed new type of "TL" lamp for large output per unit length, the "TL" double-flux lamp, is shown in *figs. 6* and *7*. This lamp also has the ordinary circular cross-section, with the exception, however, of a small protrusion made at half its length, such that the temperature at the bottom of the protrusion remains at about 40 °C, whilst all other parts of the wall become appreciably warmer. One version made on this principle has a length of 1.50 m, i.e. the same length as the "TL" 65 W lamp, and a diameter of 35 mm. With a protrusion of diameter 10 mm and depth 10 mm, the tube can be loaded with 125 W, i.e. the same load per unit length as that of the two above-mentioned American types. The current is then 1.5 A, the burning voltage 97 V, whilst the luminous efficiency after 100 hours amounts to 57 lm/W. The lamp therefore develops per unit length a luminous flux that is 1.7× as large as that of the "TL" 65 W lamp, which has an efficiency of 64 lm/W, and 2.2× as large as that of the "TL" 40 W lamp, whose efficiency amounts to 66 lm/W. The tube wall (apart from the protrusion and the regions near the electrodes) assumes a temperature of 57 °C at an ambient temperature of 25 °C. The fact that the luminous efficiency is somewhat lower than that of the "TL" 65 W lamp, although the optimum mercury-vapour pressure is maintained, is mainly attributable to the higher current density, which promotes the excitation of mercury atoms to higher energy levels.

The above design with the larger power per unit length may be applied for making lamps of various

---

[3]) J. O. Aicher and E. Lemmers, Design and characteristics of fluorescent lamps having a non-circular cross section, Illum. Engng. **52**, 579-584, 1957 (No. 11). G. R. Baumgartner, R. T. Dorsey and E. A. Linsday, Application of non-circular cross-section fluorescent lamps, Illum. Engng. **52**, 587-596, 1957 (No. 11).

[4]) J. F. Waymouth, W. Calvin Gungle, Ch. W. Jerome and F. Bitter, Very-high-output fluorescent lamps, Sylvania Technologist **9**, 102-110, 1956. J. F. Waymouth, F. Bitter and E. F. Lowry, Factors to be considered in the design of high-output fluorescent lamps, Illum. Engng. **52**, 257-261, 1957 (No. 5).

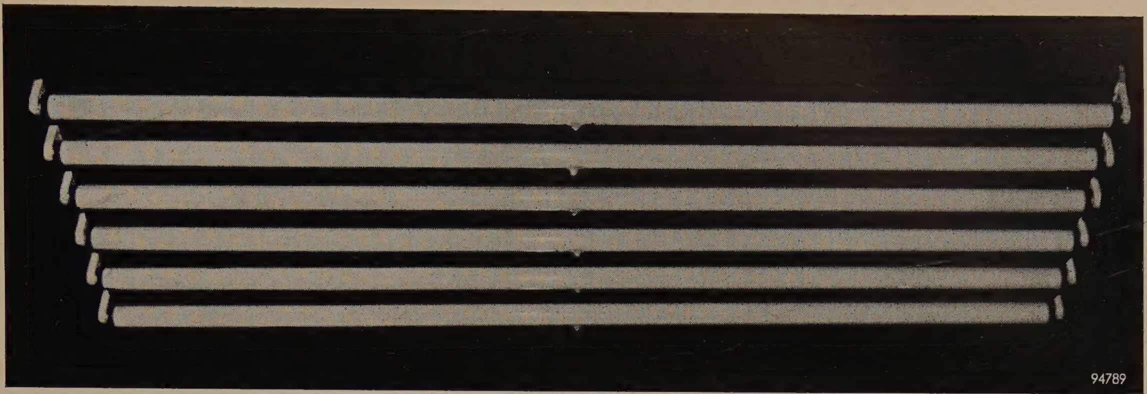

Fig. 6. A row of "TL" double-flux lamps.

power ratings (and hence lengths). The version described here, with a length of 1.50 m, has been preferred in order to attain a relatively high burning voltage. The use of neon instead of argon as ignition gas would likewise result in a higher burning voltage, but was found to be less desirable as it induced a more rapid rate of vaporization of the electrodes and hence a shortened working life. With a view to this vaporization we have also preferred a higher argon pressure, viz. ≈ 1.5 mm Hg, rather than the pressure of about 1 mm Hg prescribed for optimum efficiency.

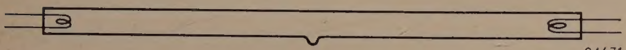

Fig. 7. Sketch of the "TL" 125 W double-flux lamp developed by Philips; the length is 1.50 m (the same length as the "TL" 65 W). There is a protrusion of depth and diameter about 10 mm on the tube half-way along its length. The temperature in the protrusion does not exceed 40 °C, so that the mercury-vapour pressure in the tube (after all the surplus mercury has condensed here) eventually assumes the optimum value.

The situation of the "cold spot" half-way along the length of the tube has the advantage of being least susceptible to the high temperature around the electrodes, so that a protrusion of such small dimensions is adequately effective. This design has the added advantage that the lamp emits light without brightness variations along its entire length. The protrusion can be made without difficulty *after* the tube has been provided with its fluorescent layer, thus avoiding any problems in depositing the latter.

After the lamp has been filled with inert gas and mercury and sealed off, the liquid mercury is distributed at random inside the lamp. Once the lamp has been delivered to site, mounted in its position and ignited for the first time, it will burn for some time at too low a voltage, because the mercury-vapour pressure is too high (there are drops of liquid mercury on the hot walls). It will take a number of burning hours before all the surplus mercury is distilled from the hot regions and condensed in the protrusion, giving the correct equilibrium mercury-vapour pressure. Only then will the burning voltage attain the required value and the lamp yield its maximum luminous flux. The period necessary for this stabilization differs from lamp to lamp, since the initial distribution of the mercury may vary a great deal.

After this stabilization period the liquid mercury will remain in the protrusion, so that almost immediately after the lamp is switched on again the maximum luminous flux is obtained. It is obvious that the lamp should only be mounted horizontally, with the protrusion in the lowermost position.

Summary. Tubular fluorescent lamps ("TL" lamps) have the highest luminous efficiency at a mercury-vapour pressure of about 5×10^{-3} mm Hg. With ordinary lamps this pressure is obtained because the temperature of the tube wall assumes a value of about 40 °C. It can be demonstrated that under this condition and for a given burning voltage the power can only be increased by making the lamp longer. However, fluorescent lamps have now been developed in which the larger part of the wall can assume a higher temperature, whilst a minor part of the area remains at 40 °C; in this case the optimum mercury-vapour pressure is retained. The "TL" double-flux lamp designed by Philips on this principle, and characterized by a small protrusion, about 10 mm in diameter and 10 mm deep, midway along the tube, has a power of 125 W at a length of 1.50 m, i.e. the same length as the ordinary "TL" 65 W lamp. The luminous efficiency of the new lamp is 57 lm/W compared with 64 lm/W for the ordinary "TL" 65 W lamp, both measured after 100 burning hours.

Erratum. *A simple apparatus for contact microradiography between 1.5 and 5 kV*, by B. Combée and A. Recourt. (Philips tech. Rev. **19**, 221-233, 1957/58, No. 7-8).
On p. 227, column (ii) of the above-mentioned article, the second sentence of the last paragraph should read:
"The experimental emulsion differs from the standard "Maximum Resolution" emulsion (type V 6005) in that it is only **4** microns thick instead of **5**, and has **5** times more grains per unit volume; the size of the AgBr grains is the same".

THE PROJECTION OF COLOUR-TELEVISION PICTURES

by T. POORTER and F. W. de VRIJER.

621.397.2:621.397.62:535.881

A projection system for monochrome television was developed in the Philips Eindhoven Laboratory over 10 years ago. Further work has now resulted in the development of apparatus for the projection of coloured television pictures on to a screen. Projectors have been built giving pictures 22 cm × 29 cm and 35 cm × 46 cm at a highlight luminance of 200 cd/m^2, and 2.25 m × 3 m at a highlight luminance of 20 cd/m^2. The latter value is about the same as that on normal cinema screens. The projectors were demonstrated before the colour-television commission of the C.C.I.R. in 1955 and 1956.

Almost all colours occurring in nature can be simulated by adding together three kinds of light, each of a suitable primary colour: red, green and blue. Colorimetric theory, as it concerns the addition of colour, was dealt with in an earlier article ^{1}) which will be referred to as I. It is possible to obtain a television picture in natural colour in the manner stated by building up each element of the picture out of appropriate quantities of light of the three primary colours. A practical method of doing so is to project a red, a green and a blue image simultaneously on to a common screen, in such a way that the three images coincide exactly. The luminance of each element of the resultant image is thus the sum of the luminances of the three corresponding elements of the primary-colour images, the colour of the resultant element being determined by the proportions of these luminances.

One obvious way of building such an apparatus would be to combine a projection type cathode-ray tube giving coloured images — working on the same principle as direct-viewing tubes for colour television — with a suitable optical system, but no projection tube for coloured images has so far been produced. However, projection tubes luminescing in each of the three primary colours do exist. A set of three projectors, one for each of the three primary colours is therefore taken as the basis of the system: the three projectors are equipped with projection tubes giving red, green and blue light.

It is of course necessary that corresponding elements of the primary-colour images should coincide on the projection screen. The correct superposition of the three images is therefore a matter requiring particular attention. One of the conditions for proper superposition is that the three projectors should be identical in design and that any differences arising in their construction should be kept as small as possible.

The primary-colour projectors

The primary-colour projectors can be designed on exactly the same lines as those for monochrome television. A projector of this kind, embodying the Schmidt optical system, was described in this journal ^{2}) and elsewhere ^{3}) in 1948. The Schmidt system combines three valuable properties, namely low optical distortion, low transmission losses and large aperture. In its simplest form the system comprises the arrangement shown diagrammatically in *fig. 1a*. However, as stated in the article referred to in footnote ^{2}), the alternative arrangement shown in fig. 1*b* has been used in home projection receivers. Here the light beam is "folded" by means of a plane mirror M_2, which is placed at

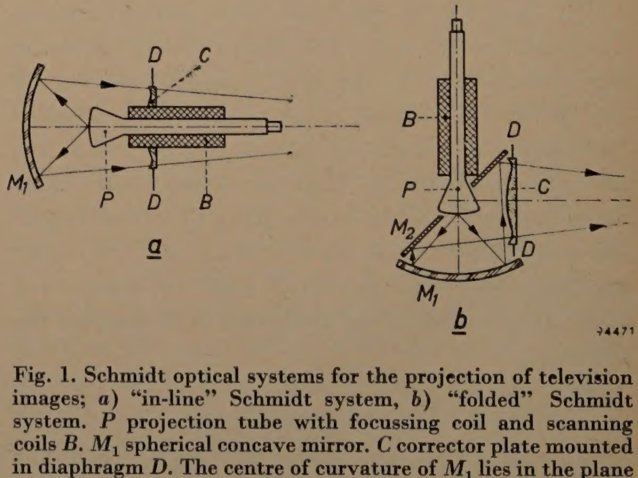

Fig. 1. Schmidt optical systems for the projection of television images; *a*) "in-line" Schmidt system, *b*) "folded" Schmidt system. *P* projection tube with focussing coil and scanning coils *B*. M_1 spherical concave mirror. *C* corrector plate mounted in diaphragm *D*. The centre of curvature of M_1 lies in the plane of *D* in the case of (*a*) and in the image of *D* given by plane mirror M_2 in the case of (*b*).

---

^{1}) F. W. de Vrijer, Fundamentals of colour television, Philips tech. Rev. **19**, 86-97, 1957/58 (No. 3).

^{2}) P. M. van Alphen and H. Rinia, Projection-television receiver, I. The optical system for the projection, Philips tech. Rev. **10**, 69-78, 1948/49.

^{3}) H. Rinia, J. de Gier and P. M. van Alphen, Home projection television, I. Cathode-ray tube and optical system, Proc. Inst. Rad. Engrs. **36**, 395-400, 1948.

an angle of 45° to the principal axis. This arrangement allows the set to be constructed more compactly and to be enclosed in a dust-proof box. When space is availabe, however, there is no reason why the "in-line" optical system shown in fig. 1*a* should not be used [4]).

Superposition of the three primary-colour images

There are several possible ways of arranging for the primary-colour images to coincide on the projection screen. A general distinction may be made between arrangements whereby the three projectors, from an optical point of view, are effectively coincident (all done by mirrors), and all other arrangements.

Three projectors effectively at the same point

In theory superposition errors are absent if one can somehow place the projectors such that the three images are projected, as it were, from one point. *Fig. 2* shows how this may be done with the aid of two dichroic mirrors as discussed recently in this journal [5]). Mirror *r* reflects red light and passes green and blue; mirror *b* reflects blue and passes red and green. Green light has to go through both mirrors, the proportion transmitted being between 70% and 80%.

The crossed mirrors may be mounted with the line of intersection either horizontal or vertical. If the line of intersection is horizontal the three projectors will have to be in a vertical plane, and this has the advantage that colour variations over the area of the projected picture are reduced to a minimum. The variations arise because the light beams do not all strike the mirrors at the same average angle; with the line of intersection horizontal, the angle over which variations occur is subtended by the lesser dimension of the picture, namely its height. However, if the apparatus is for projecting large pictures, care must be taken not to build it too tall, otherwise it will interfere with part of the audience's view of the screen. This problem arises because in order to keep down the dimensions of the main optical system, the projectors have to be placed as close to the sreen as possible, i.e. in front of the viewers. It has proved possible to keep the height of the projection apparatus down to 1.35 m as shown in *fig. 3*, which gives the dimensions of the first of the large-screen colour television projectors built in this laboratory (photograph in *fig. 4*).

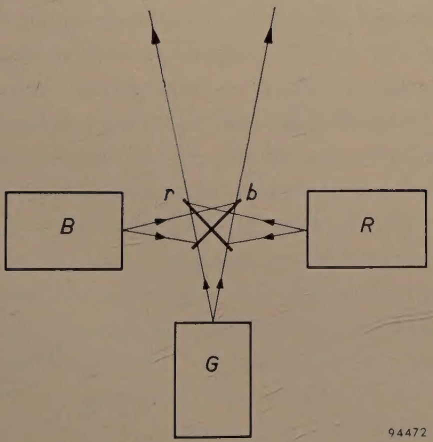

Fig. 2. Superposition of three primary-colour images by means of crossed dichroic mirrors (*r* and *b*). Mirror *r* reflects the red light from *R* and passes the green from projector *G* and the blue from projector *B*. Mirror *b* reflects blue light and passes red and green.

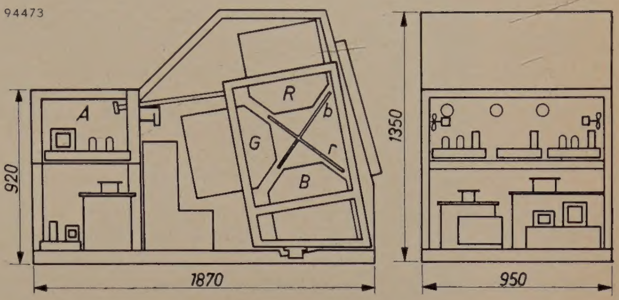

Fig. 3. Sketch of the first large-screen colour-television projector constructed at Eindhoven (see also fig. 4); it gives a picture measuring 2.25 m × 3 m (≈ 7½′ × 10′). *r* and *b* are crossed dichroic mirrors with their line of intersection horizontal. This means that *R*, *G* and *B*, the primary-colour projectors, are mounted in a vertical plane; despite this it was possible to limit the overall height of the apparatus to 1.35 m. Compartment *A* contains the supply unit. The dimensions shown are in mm.

If the mirrors are mounted with their line of intersection vertical and the primary-colour projectors are accordingly placed in a horizontal plane, it is easier to keep down the height of the apparatus but there will be greater colour variations in the projected picture.

Much depends on whether the crossed mirrors are combined with "in-line" or "folded" Schmidt optical systems. In the first kind of Schmidt system the projection tube, surrounded by the focussing and scanning coils, protrudes through an opening in the corrector plate (fig. 1*a*). In order that the tube and coils should block the path of the reflected light as little as possible, they have to be located outside the crossed mirrors. These latter have therefore to be set up some distance away from the corrector plates (in fig. 1*a* they would be mounted to the right of the foot of the tube), in a place where the re-

---

[4]) J. Haantjes and C. J. van Loon, A large-screen television projector, Philips tech. Rev. **15**, 27-34, 1953/54.

[5]) P. M. van Alphen, Philips tech. Rev. **19**, 59-67, 1957/58 (No. 2).

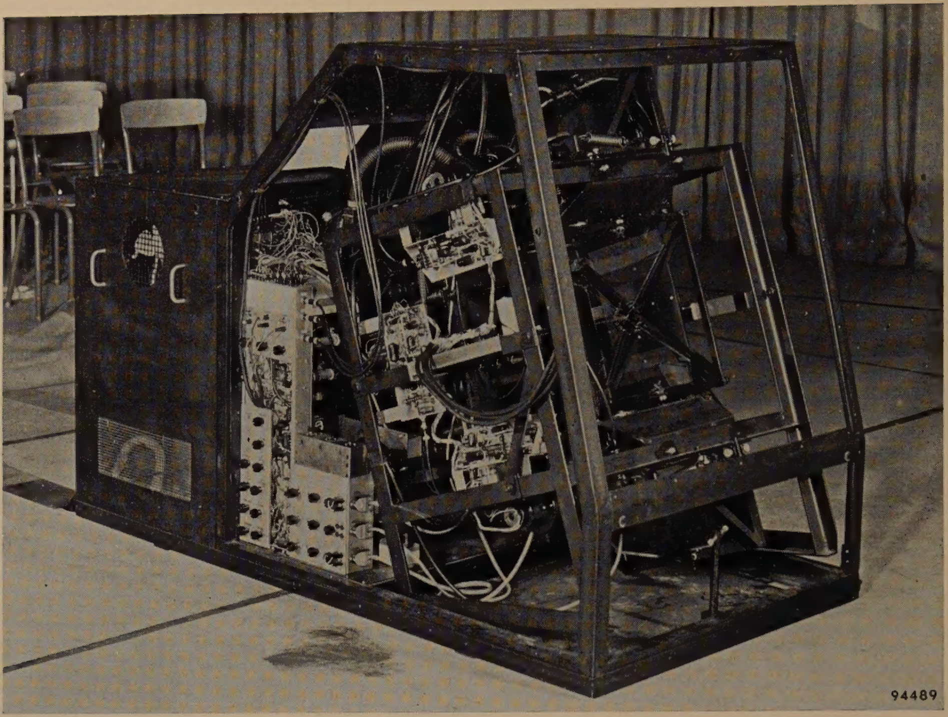

Fig. 4. Photograph of the colour-television projector sketched in fig. 3. The size of the projected picture is 2.25 m × 3 m (≈ 7½′ × 10′) and its maximum luminance is about 10 cd/m^2. Electrical adjustments are carried out from a control desk (not shown in the photograph).

flected beams have a fairly large diameter. In consequence, the mirrors have to be bigger than they are in "folded" systems (fig. 1*b*), where the crossed mirrors can be set up close to the corrector lenses. The "in-line" optical system also necessitates special arrangements for inserting and withdrawing the CRT; for example, it might be necessary to design the concave mirror in such a way as to allow of dismantling.

Projectors using horizontally intersecting dichroic mirrors have been built, and have given good results. In general, however, designs embodying dichroic mirrors have two disadvantages. The first is a loss of brightness and contrast, due to the large number of reflecting and absorbing surfaces in the path of the beams, especially if these are "folded". The second disadvantage is a loss of sharpness due to the difficulty in achieving a completely stress-free mounting of the mirrors. In consequence, ways have been sought of superimposing the three primary colour images without the aid of dichroic mirrors. This line of enquiry has led to arrangements whereby the three primary-colour images are *not* projected effectively from the same point. This necessarily results in certain superposition errors and, in general, some compensation of these must be sought, using special corrective measures.

Projectors not effectively at the same point

a) The projectors are placed at the apexes of an equilateral triangle. Of all the different arrangements that are possible, this involves the smallest errors of superposition; the triangular arrangement will therefore be attractive where it is not desired to undertake any corrective measures. However, such measures can only be dispensed with if the optical magnification is large — the errors diminish in relation to the picture size as the magnification increases. Correction of the errors, necessary where magnification is not so large, is more complicated in this arrangement than in those now to be discussed.

b) The projectors are arranged side by side. We may distinguish between two cases: (1) where the three projectors are parallel to one another, their axes being perpendicular to the projection screen, and (2) where the outside projectors are inclined inwards slightly.

The following observations apply equally well, *mutatis mutandis*, to arrangements whereby the three projectors are mounted one above the other. Such arrangements are less desirable, however, because they occupy a greater height.

b1) The three projectors are side by side with their axes parallel. Each throws a rectangular image on to the screen and, in theory, the projected images can be made to coincide by displacing the luminescent images on the two outside tubes electrically. If the luminescent images are to be displaced from the central position on the tube screen it is necessary that they should not occupy the whole of its area. Thus only part of the tube screen is utilized, with the consequence that stronger magnification is necessary and that the highlight luminance on the projection screen will be lower than the maximum obtainable. In addition, vignetting will occur, owing to the fact that the central ray passes obliquely through the optical system. It is a condition for success that the deflection coils should be so designed that the images on the projection screen are completely free from distortion. This ideal cannot be approached closely enough in practice, and so the method can only be used where the magnification is very large and where, in consequence, the outside CRT screen images need only be displaced slightly.

b2) The outside projectors are pointed inwards (*fig. 5a*) in such a manner that their optical axes intersect in the centre of the projection screen. The deflection coils are adjusted such that the vertical centre lines of the separate images coincide (along *MM'* in fig. 5*b*). The result is that, for the images from the outer projectors the magnifications are not equal in the left and right halves of the picture, giving rise to trapezium shaped images. By introducing an electrical correction into both the line and frame scanning of the outside tubes (how this is done will be discussed below) the images from these two projectors can be made to coincide with the rectangular image projected by the centre projector.

Prior to correction, with the three projectors positioned in the best possible manner, the superposition errors arising in the corners of our projected pictures were as follows. In a picture measuring 2.25 m × 3 m the error was six times the inter-line separation; in a picture measuring 22 cm × 29 cm the error was thirty times the inter-line separation. Both cases refer to a raster of a 625 lines.

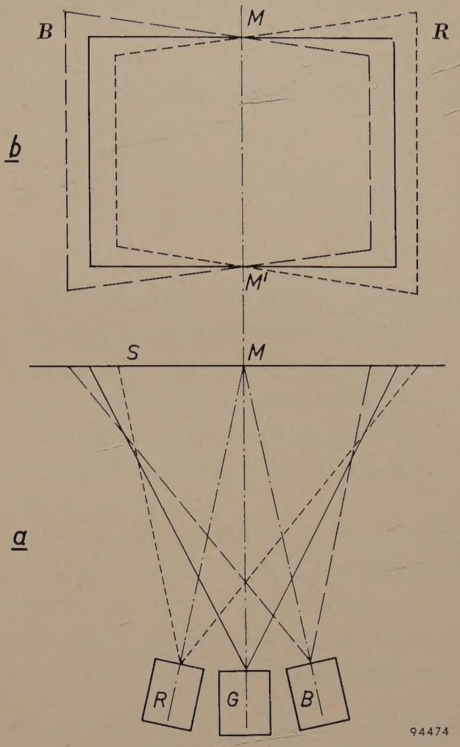

Fig. 5. *a*) Arrangement whereby the three primary-colour projectors *R*, *G* and *B* are placed side by side, with the two outer ones inclined inwards at an angle such that the vertical lines through the centres of the three images (*MM'* in diagram *b*) coincide.
b) In consequence, the red and blue images suffer from trapezium distortion.

Since the axes of projectors *R* and *B* are not now perpendicular to the projection screen (fig. 5*a*) there ceases to be a linear relationship between the horizontal movements of the red and blue spots on the screens of the outside tubes and the movements of their respective projected images. In order to give the spots on the projection screen a constant horizontal velocity, the line scanning current must be given the form indicated in *fig. 6a*. This means adding correction currents to the normal line scanning currents of the outside projection tubes. The two correction currents are, of course, equal and opposite; hence only one current has to be generated and to be passed in the appropriate

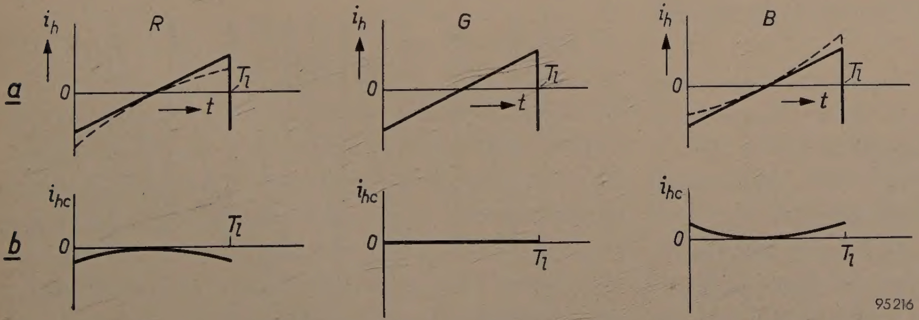

Fig. 6. *a*) Waveform required (dashed curves) for the line scanning current (i_h) in primary-colour tubes *R*, *G* and *B* (mounted as in fig. 5*a*) in order that linearity be restored to the movement of the three spots across the projection screen. T_l is the line period.
b) To obtain the above waveforms, the linear sawtooth currents in *R* and *B* (full lines in *a*) must have correction currents i_{hc} added to them; the two correction currents are equal and opposite.

direction through the scanning coil of each of the outside tubes. Prior to this correction, the three images on the projection screen have the outlines shown in *fig. 7a* after applying the above correction, they take on the shapes shown in fig. 7*b*.

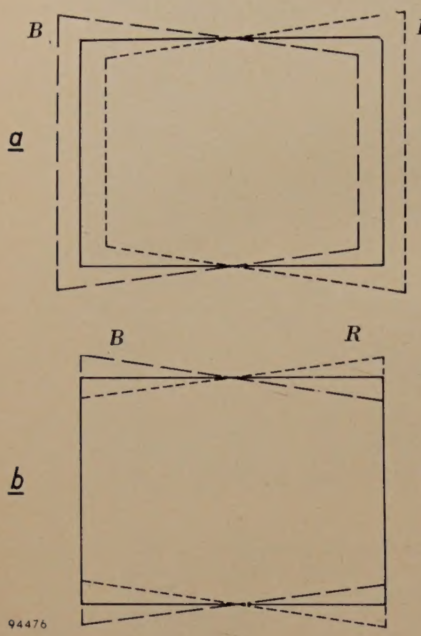

Fig. 7. *a*) Outlines of the three primary-colour images on the projection screen prior to correction (cf. fig. 5*b*).
b) Application of the correction illustrated in fig. 6 brings the vertical edges of the three images into coincidence. To get complete coincidence of the images, correction of the vertical (frame) scanning is further necessary — see fig. 8.

The red and blue images on the projection screen are still of trapezium shape; to make them coincide with the rectangular green image, the frame scanning must also be subjected to a correction. From a glance at the outline of, say, the blue image in fig. 7*b*, it will be clear that the vertical scan has to be shortened on the left and lengthened on the right, in the rhythm of the line frequency. The frame scanning current of the blue CRT must therefore have a correction current of the following description superimposed upon it.

(i) While the beam is at the top of the screen the correction current must go from negative to positive as the beam swings from left to right.

(ii) When the beam is half way down the screen the correction current must be zero.

(iii) While the beam is at the bottom of the screen the correction current must go from positive to negative as the beam swings from left to right.

(A "positive" correction current is here taken to mean a deflection towards the top of the projected image.)

The correction current must therefore have the shape drawn in *fig. 8a*, and it might be obtained by multiplying a sawtooth of frame frequency (fig. 8*b*) by a sawtooth of line frequency (fig. 8*c*); how it is actually done will be described later.

At the same time the red CRT must also be supplied with a correction current of the same magnitude but of opposite direction. For the corrections to the vertical scanning for both red and blue tubes, therefore, it will again suffice to generate a single correction current.

It should be observed for the sake of completeness that the addition of correction currents is not the only way of modifying the rasters of the outside tubes; it is possible in theory to give the scanning coils a shape different from the normal. But this involves two complications: first, electron-optical

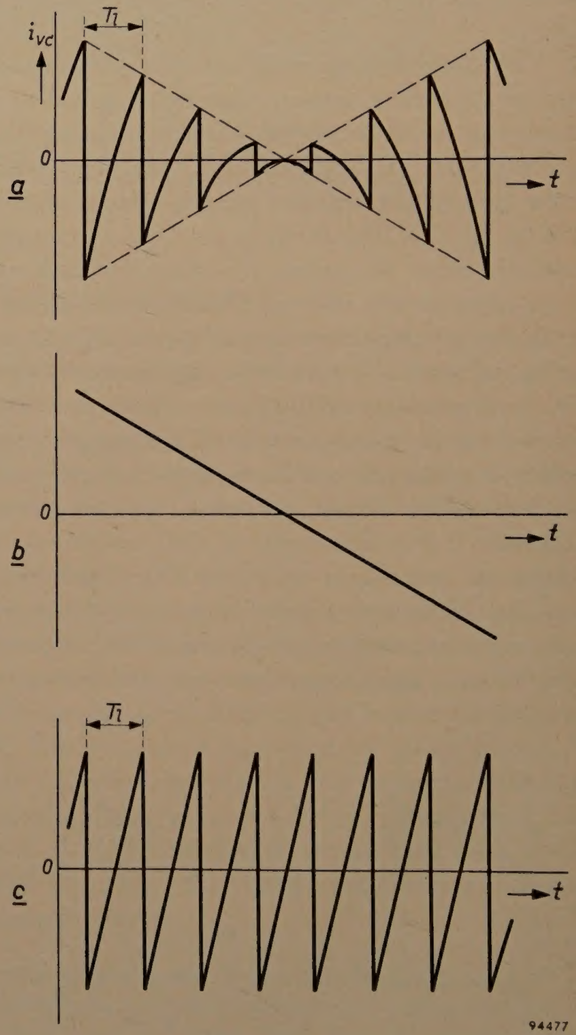

Fig. 8. Trapezium correction. *a*) Waveform of correction current i_{vc} that has to be added to the frame scanning current of the right-hand projector (*B* in fig. 5*a*); the left-hand projector requires correction with a current of the same magnitude but of opposite sense. T_l is the line period. The function drawn in diagram (*a*) is the product of the sawtooth (*b*) of frame frequency, and the sawtooth (*c*) of line frequency.

errors may be introduced and, secondly, the coils in question are difficult to manufacture reproducibly. The method involving special scanning coils is therefore less attractive than that utilizing correction currents.

Optical system of the equipment

The dimensions of the optical systems and projection tubes are determined by what is required of the projected picture as regards size and peak luminance, and also by the luminous efficiency of the phosphors used for the tube screens. Phosphors capable of taking the very high loads that occur and with colour points close to the primary colours laid down in the N.T.S.C. (U.S.A. National Television System Committee) system are listed in *Table I.* Luminous efficiencies in lumens per watt are also indicated.

Table I. Data on the phosphors used.

Primary colour	Composition of phosphor	Coordinates of the colour point x	Coordinates of the colour point y	Luminous efficiency lm/W
Red	$(Zn,Be)_2SiO_4$-Mn (with Wratten filter 25)	0.670	0.330	$\eta_r = 2.5$
Green	Zn_2SiO_4-Mn	0.195	0.720	$\eta_g = 21$
Blue	$(Ca,Mg)SiO_3$-Ti	0.160	0.125	$\eta_b = 2.5$

Projection equipment without dichroic mirrors

For equipment not employing dichroic mirrors, the colour points of the phosphors are the same as those of the primary colours forming the projected picture. In order to obtain standard white C (see [1]), fig. 8) from a combination of these primary colours, the luminance values of the primary colours have to be in the following proportions:

$$L_r : L_g : L_b = 29 : 51 : 20.$$

Accordingly, the projection tube screens must dissipate powers in the proportions:

$$P_r : P_g : P_b = \frac{L_r}{\eta_r} : \frac{L_g}{\eta_g} : \frac{L_b}{\eta_b} = 53 : 11 : 36.$$

We see that the red tube screen has to dissipate the highest power. In a normal colour-television picture, white features are responsible for the heaviest loading of all three of the tubes; hence the maximum loading the red tube can be allowed to undergo sets a limit to the maximum brightness that can be obtained in the projected picture. If therefore the three projectors are identical in design, the design of the apparatus as a whole will have to be based on the luminance that the red light contributes to the brightest white parts of the projected picture. If this is desired to have a highlight luminance of $L'_{\max}$, the red contribution will be

$$L_r'{}_{\max} = \frac{L_r}{L_r + L_g + L_b} L'_{\max} = 0.29\, L'_{\max}. \qquad (1)$$

It has been found that the mean luminance of an average television picture amounts to about a third of the peak value. The red tube must therefore supply a total luminous flux of

$$\Phi_r = \frac{\pi b'h'}{\tau_1 \tau_2 a^2 \mu} \frac{L_r'{}_{\max}}{3} \text{ lumen}, \quad . \ . \quad (2)$$

where

b' is the width and h' the height (in metres) of the picture on the projection screen;

a the numerical aperture of the projector;

μ the "gain" given by the projection screen (due to directionally selective reflection);

τ_1 the masking coefficient (masking effect of CRT in optical system);

τ_2 the optical transmission coefficient of the system;

$L_r'{}_{\max}$ the maximum luminance in cd/m² of the red image on the projection screen.

The electrical power that the red tube must dissipate in order to supply the above value of luminous flux is

$$P_r = \frac{\Phi_r}{\eta_r}. \quad . \ . \ . \ . \ . \ . \quad (3)$$

If p is the maximum power that can be dissipated per unit area of the tube screen, the area bh of the image on the latter must satisfy

$$b\,h = \frac{P_r}{p}. \quad . \ . \ . \ . \ . \ . \quad (4)$$

The aspect ratio $b : h$ is laid down at 4 : 3, and this allows us to work out b, h and the diagonal of the picture which should not, of course, exceed the diameter of the fluorescent screen. This gives us the magnification that has to be effected in the optical system of the projector:

$$N = \frac{b'}{b}.$$

Straightforward geometrical-optical reasoning shows that the following relationships must exist between the magnification N, the distances x and x' of object and image from the focus F', the focal length f' and the distance Δ' between the corrector plate and the screen (see *fig. 9*):

$$|N| = \left|\frac{x'}{f'}\right| = \left|\frac{f'}{x}\right| = 1 + \frac{\Delta'}{f'}. \quad . \ . \quad (5)$$

For a given magnification, f' would have to be

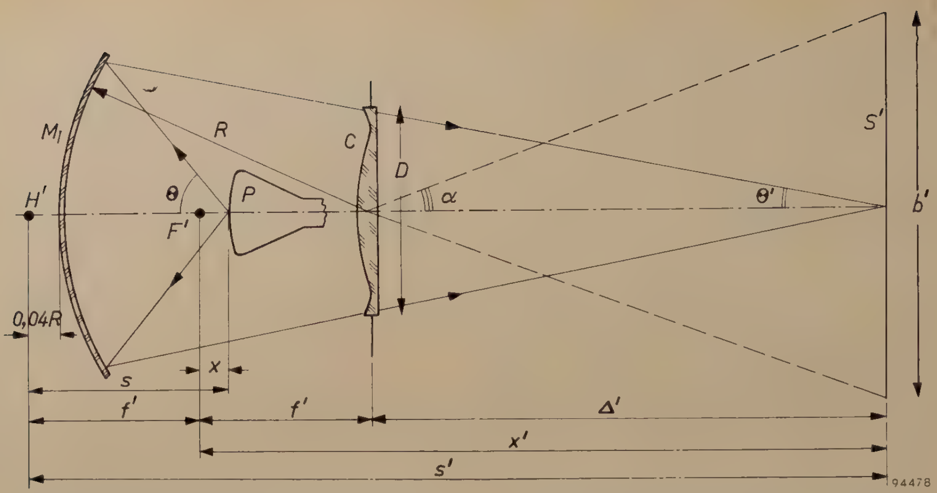

Fig. 9. Schmidt optical system of the "in-line" type. P projection tube. M_1 concave mirror of radius R. C corrector plate of diameter D. S projection screen, the image on which is of breadth b'. F' focus of mirror plus corrector plate. H' pole of mirror plus corrector plate.

increased in direct proportion to Δ', and so also would all the principal dimensions of the optical system. The distance Δ' should therefore be kept as short as possible (this is why the apparatus is set up in front of the viewers). However, there is also a lower limit to Δ', since, as the picture angle 2α increases (this being the angle subtended by the width of the projected picture at the centre of the corrector plate — see fig. 9), optical aberrations increase and, apart from that, an increasing fall-off in brightness between the centre and edges of the screen picture becomes evident. There is therefore a certain picture angle $2\alpha_{\max}$ at which these effects are still tolerable and which must not be exceeded. Accordingly, the minimum distance between the corrector plate and projection screen is then

$$\Delta'_{\min} = \frac{\frac{1}{2}b'}{\tan \alpha_{\max}} \quad \ldots \ldots \quad (6)$$

We can now obtain the focal length from (5) and (6):

$$f' = \frac{\Delta'_{\min}}{|N|-1} \quad \ldots \ldots \quad (7)$$

The radius of curvature R of the concave mirror is approximately $2f'$.

The diameter D of the corrector plate is worked out as follows. We see from fig. 9 that $D = 2\Delta' \tan \Theta'$. Furthermore, $\sin \Theta' = (\sin \Theta)/|N| = a/|N|$. The angle Θ' is so small that $\tan \Theta' \approx \sin \Theta'$. Hence,

$$D \approx \frac{2a}{|N|}\Delta' \quad \ldots \ldots \quad (8)$$

By way of illustration, a design study will now be outlined for an equipment to project a coloured television picture measuring 2.25 m × 3 m and having a maximum luminance of 20 cd/m². We assume that the picture is projected onto a "beaded" screen having a "gain" of $\mu = 2.8$. A practical value for the numerical aperture is $a = 0.7$. The product $\tau_1\tau_2$ can be assumed to be 0.5 and we can take p to be 4000 W/m². Formula (1) gives the maximum luminance of the projected red image:

$$L_r{}'_{\max} = 0.29 \times 20 = 5.8 \text{ cd/m}^2.$$

The following values are obtained successively from (2), (3) and (4):

$$\Phi_r = 59 \text{ lm},$$

$$P_r = \frac{59}{2.5} = 24 \text{ W},$$

$$b\,h = \frac{24}{4000} = 6 \times 10^{-3} \text{ m}^2.$$

From these we work out the dimensions of the image on the CRT screen:

$$b = 9 \text{ cm};\ h = 6.7 \text{ cm};\ \text{diagonal} = 11.2 \text{ cm}.$$

A projection tube with dimensions of the MW 13-38 (which has a screen of diameter 13 cm) can therefore be used.

The magnification N is equal to $b'/b = 300/9 \approx 33$. In a Schmidt optical system the maximum picture angle $2\alpha_{\max}$ is round about 30°, and on this basis we can determine the minimum distance between corrector plate and projected picture from (6):

$$\Delta'_{\min} = \frac{\frac{1}{2} \times 3}{\tan 15^\circ} = 5.60 \text{ m}.$$

Formula (7) gives the focal length:

$$f' = \frac{560}{33-1} = 17.5 \text{ cm}.$$

The concave mirror must therefore have a radius of curvature of $R \approx 2f' = 35$ cm. The periphery of the mirror is usually given a diameter approximately equal to R; with a smaller mirror, differences of illumination over the projection screen area would be too apparent.

Finally, the diameter of the corrector plate is obtained from (8):

$$D \approx \frac{2 \times 0.7}{33} \times 560 \approx 24 \text{ cm}.$$

Projection equipment embodying dichroic mirrors

The foregoing applies to an equipment that does not embody dichroic mirrors. The design procedure for a projector that does employ such mirrors is similar, except that the design must be based on a different set of relationships between L_r, L_g and L_b, the reason being that the selective transmission and reflection of the dichroic mirrors causes the colour points of the primary colours to shift. In addition, transmission losses in the mirrors must be taken into account in the calculation of the electrical powers that must be dissipated by the projection tubes. As already stated, the "folded" optical system is preferred where dichroic mirrors are to be used; but such a system has a lower transmission coefficient. If the projectors are to have the same dimensions as in the foregoing, the overall result of all this is that highlight luminance of the projected picture will be reduced by roughly 50%. Projectors designed on the above lines and used in combination with dichroic mirrors will therefore be able to produce a maximum luminance of about 10 cd/m² on the projection screen.

Table II gives the dimensions of the four equipments built in this laboratory. Column 1 relates to a projector corresponding roughly to the example worked out above.

Mechanical details of the optical systems

The projection tube, complete with focussing and deflection coils, must be mounted in its optical system in such a way as to enable *optical focussing* to be carried out by altering the position of the tube with respect to the concave mirror. For this purpose it must be possible to move the tube forward and backward along its own axis and also to turn it about two axes perpendicular to each other and to the axis of the tube, running through the centre of the tube screen. *Fig. 10* shows how this is done in the projector depicted in fig. 4. The projection tube P, together with coils D and F, is suspended in a yoke B consisting of a flanged plate holding the tube assembly. Two threaded holes in the plate carry threaded rods I whose ends rest in recesses U and V, being retained by tension springs between the plate and the chassis. The third point of support is provided by an angle bracket fixed to the plate, resting on a bolt (W) threaded in a chassis member. The points U and V lie on the horizontal line passing through the centre of the tube screen. If the adjusting screws marked I are turned to the same extent in the same direction, the tube moves forward or back; if they are turned to the same extent in opposite directions, it turns about the vertical axis through the centre of its screen. Adjusting the knob II on W causes the tube to turn in a vertical plane, about the axis UV. These operations, each of which is substantially independent of the others, allow the whole area of the projected image to be brought into focus.

Table II. Data on the Schmidt optical systems used in the four colour-television projectors constructed.

	1	2	3	4
Dichroic mirrors	no	yes	yes	yes
Type of system	"in-line"	"folded"	"folded"	"folded"
Picture on projection screen:				
Height h' **)	2.25	2.25	0.35	0.22
Breadth b' **)	3.00	3.00	0.46	0.29
Max. luminance L'_{max} (cd/m²)	20	10	200	200
Contrast ratio	35	25	25	25
Definition *)	600	425	450	500
Screen "gain" μ	2.8	2.8	7	7
Diam. of tube screen **)	0.13	0.13	0.06	0.06
Radius of curvature R of concave mirror **)	0.40	0.40	0.20	0.20
Focal length f' **)	0.208	0.208	0.104	0.104
Diameter D of corrector plate **)	0.28	0.25	0.125	0.125
Projection distance Δ' **)	6	6	0.825	0.645
Magnification $\|N\|$	31	31	9.2	7.4

*) Number of lines; determined with an RMA test plate.
**) In metres.

Vignetting is an important point in the design of optical systems. The endeavour must be to keep the amount of vignetting the same to the left and right, so that both halves of the projected image are equally bright. In an apparatus embodying dichroic mirrors, the images on the three tube screens are in different orientations with respect to their optical systems, owing to the various mirror inversions; if therefore local colour variations are to be avoided, it is particularly important that the vignetting of the optical systems should be the same at the top and bottom of the picture.

We shall deal later with the arrangements for altering the position of the coils. It may be merely observed at this point that interaction between the focussing and scanning coils may lead to an error in superposition that cannot be corrected; this error takes the form of differences in curvature between horizontal and vertical lines in the three primary-colour images. Such interaction must therefore be obviated, one way of doing so being to fit a copper ring and a ring of material that is a good magnetic conductor between the focussing and the deflection coils.

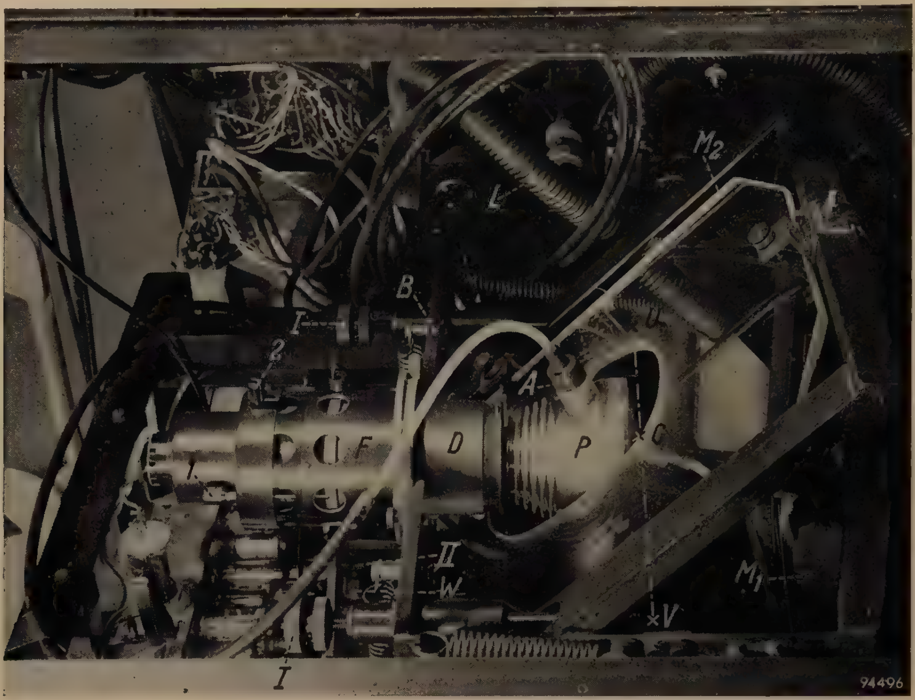

Fig. 10. One of the primary-colour projectors of the large-screen apparatus shown in fig. 4. *P* is the projection tube, *A* its anode connection, *D* the scanning coils and *F* the focussing coil. M_1 is the concave mirror, M_2 a plane mirror inclined at 45°. *L* is a flexible pipe through which cooling air is blown against the window of the tube. Part of the video amplifier is visible below, on the left. Tube and coils are suspended in a yoke *B* supported at points *U*, *V* and *W*. By turning the screws *I-I* both in the same direction the tube is moved backward or forward along its own axis; turning them in opposite directions causes the tube to swing laterally about the vertical line through the centre *C* of its fluorescent screen. Turning screw *II* causes the tube to turn about the horizontal line *UV* passing through *C*. Controls *1* and *2* are for moving the focussing coil (see below).

Circuits and adjustments for obtaining superposition of the primary-colour images

If the three primary-colour images are to be brought into correct superposition on the projection screen, the apparatus must allow of a number of adjustments and corrections, some of which have already been mentioned.

1) In an apparatus with converging projectors (fig. 5) *trapezium correction* (figs. 6 and 8) will be necessary to turn the two images with that shape into rectangular ones.

2) The three reactangular images must be of the same size; if must therefore be possible to control the *amplitude* of the scanning currents.

3) It may be necessary to correct the *linearity* of the scanning, in order to ensure movement of the three spots across the projection screen at the same speed.

4) *Displacements* of the three images will be necessary, in order to make their centres coincide.

5) *Rotational alignment* of the images will be necessary, in order to bring their longer edges into parallelism.

In addition to all this it will be necessary to take into account the *spread* in the electrical and mechanical properties of certain components: there will be differences in the deflection sensitivity of the projection tubes, in the position of the electron gun in relation to the tube axis, in the accuracy with which the angle between the two scanning directions approximates to 90° for the different sets of coils, and so on.

Most of the corrections can be incorporated in the scanning arrangements, and we shall therefore start by discussing the appropriate circuits.

The scanning circuits

Apart from the necessary corrections the deflection of the electron beams of the three projection tubes must be identical. Hence, if the three scanning units were exactly similar and if the three tubes had exactly the same deflection sensitivity, the scanning currents would likewise have to be exactly equal for each of the two scanning directions. In order to ensure from the outset that the said currents will be as nearly equal as possible, it is advisable to take them from a common generator for each scanning direction, rather than separate ones for each CRT. With separate sawtooth generators, the free oscillations that might arise in the deflection coils and transformer windings would be independent of one another, and this would render the exact superposition of the three primary-colour images impossible. Moreover, changes in the properties of the scanning generator tubes would, in the long run, give rise to discrepancies in the scanning current amplitudes, and hence to dimensional differences in the primary-colour images. Furthermore, such a method would be expensive.

The common scanning generator can be made to supply the three deflection coils connected either in series or in parallel. It might be thought that, with the series arrangement, exactly the same current would flow through the three coils. However, each coil has a stray capacitance in parallel with it, so that the arrangement in fact constitutes three oscillatory circuits in series, each able to oscillate at its natural frequency. In general, the three frequencies will not be the same and discrepancies will again arise in the scanning currents, resulting in superposition errors. Another objection is that two of the three coils carry high peak voltages with respect to earth, which might give rise to difficulties.

If the coils are in parallel, the same voltage is across all three and hence it is impossible for them to oscillate independently of one another. By inserting a variable impedance in series with each coil, the amplitude and linearity of the current through it can be adjusted to some extent. It is very easy to introduce other corrections that may be necessary, as will presently be evident. For these reasons it is only the parallel arrangement that is used.

Skew-correction

A scanning unit should deflect the beam in two directions with an angle of exactly 90° between them. In practice there is a certain amount of spread in this angle as exhibited by different deflection yokes. Any deviation from 90° manifests itself on the receiver screen as a departure from exact perpendicularity between the vertical and horizontal lines of the picture. The deviation is so slight in normal units that its effect is unnoticeable in monochrome television. In colour television, on the other hand, the deviations may be troublesome because they may differ in magnitude and direction as between the three primary-coulour images. To obviate them, either scanning units must be used that have been built with extreme care, or the fault must be corrected by electrical methods.

In order to correct skewness in the projected image electrically, the line scanning coils are injected with a correction current that is proportional to i_v, the frame scanning current. Since the frequency of i_v is so low that the scanning coils respond to i_v practically as resistances, it will suffice to introduce variable and reversible voltages, proportional to i_v, in series with the coils. These voltages should preferably be obtained from separate sources, in order to prevent the adjustments affecting one another. This skew correction only needs to be provided for in two of the three primary-colour projectors.

Adjustment of amplitude

The output circuit of the common sawtooth generator for the frame scanning is as shown in *fig. 11*. As already stated the frame scanning coils may be regarded as behaving as resistances with regard to i_v. They also possess some inductance, however, and the linearity of the sawtooth current would not be preserved if its amplitude were adjusted with the aid of a variable resistor alone, placed in series with the coil. The ratio of the resistance of the combination to its inductance would vary, and so would the shape of the current, causing errors of superposition. If therefore the shape of the sawtooth supplied to the three CRTs is to be kept uniform, a small variable inductance must be placed in series with each coil (fig. 11).

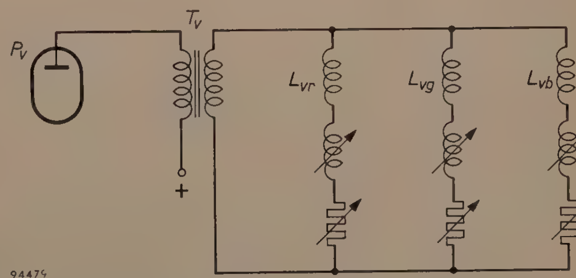

Fig. 11. Adjustment of the amplitude of the frame scanning currents. L_vr, L_vg and L_vb are the frame scanning coils of the red, green and blue tubes respectively. P_v is the output tube of the common sawtooth generator. In series with each of the coils are a variable resistor and a variable inductance, the purpose of the latter being to keep the ratio between total resistance and inductance constant.

With the line scanning coils it is otherwise; these behave more or less as inductances with regard to i_h, the current flowing through them. Consequently, the adjustment of amplitude must be effected by means of a variable inductance in series with the coil, a small variable resistance also being present, so that the ratio of resistance to total inductance can be kept constant. It is desirable that the loading of the horizontal time-base should be kept as nearly constant as possible; accordingly, a potentiometer arrangement of inductances, as shown in *fig. 12* is to be preferred.

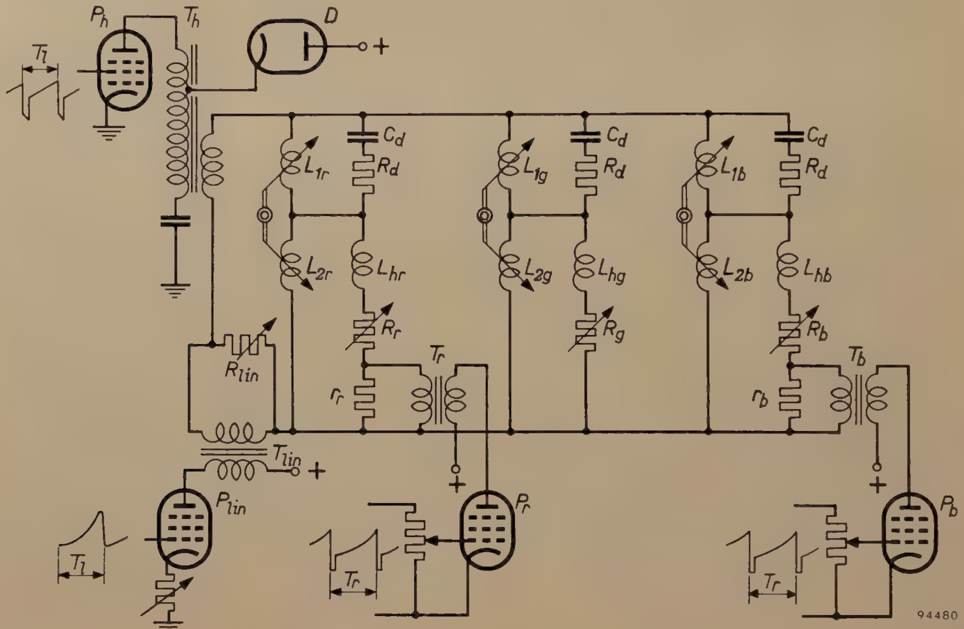

Fig. 12. Adjustment of the amplitude of the line scanning currents. L_{hr}, L_{hg} and L_{hb} are the line scanning coils of the red, green and blue tubes respectively. P_h is the output tube of the common sawtooth generator, T_h transformer. D series efficiency diode (usual in line time-bases). L_{1r}-L_{2r}, L_{1g}-L_{2g} and L_{1b}-L_{2b} are potentiometrically connected variable inductances. R_r, R_g and R_b are variable resistances allowing the ratio between total inductance and resistance to be kept constant. The R_d-C_d networks are for damping free oscillations. The sawtooth current delivered by T_h is rendered linear via pentode P_{lin}, transformer T_{lin} and resistor R_{lin}, the linearity control being the cathode resistor of P_{lin}. A correction current proportional to i_v is fed to the red and blue CRTs via P_r-T_r-r_r and P_b-T_b-r_b respectively (for skew-correction). T_l = line period. T_r = frame period.

It may also be seen from fig. 12 how the skew correction is effected in a large-screen projector. Transformers T_r and T_b are fed, independently of each other, from pentodes P_r and P_b respectively, these tubes being controlled by an adjustable fraction of the sawtooth voltage on the grid of the frame-scan output tube. Resistors r_r and r_b thus have voltages across them which have the same shape as i_v, and which, by correcting the current i_h flowing through line-scanning coils L_{hr} and L_{hb}, serve to correct skewness in the projected images.

A further voltage of sawtooth shape and line frequency is fed in via pentode P_{lin} and transformer T_{lin}; it is controlled by means of the cathode resistor of P_{lin}. This allows for the compensation of any lack of linearity in the current from the common sawtooth generator, and is effective for the line scanning of all three projection tubes.

The coarse adjustment of scanning amplitude is carried out elsewhere in the line scanning generator, one control serving for all three scanning coils. The same applies to the frame scanning generator.

Trapezium correction

In apparatus with the arrangement of projectors shown in fig. 5, the frame and line scanning of the two outer CRTs must be made subject to correction, as already pointed out (figs. 6, 7 and 8).

A circuit for superimposing a correction current on the *frame* scanning current appears in *fig. 13*. The uncorrected sawtooth current arrives via transformer T_v, the correction current via transformer T_{vc}. The circuit is designed in such a way as to maintain the correct relative direction of the two currents and to prevent mutual interference between the generators producing them.

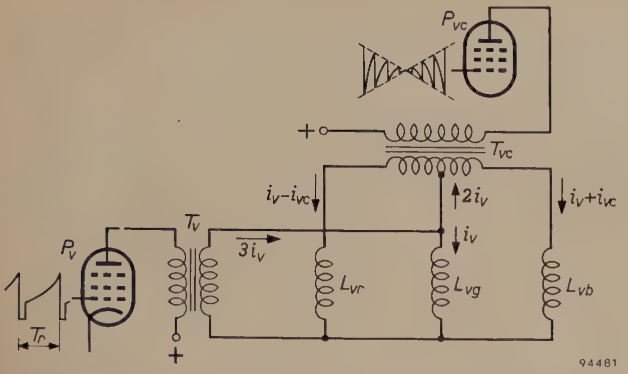

Fig. 13. Circuit for adding i_{vc}, the current for correcting trapezium distortion, to the frame scanning current i_v in the inductances L_{vr} and L_{vb}. The correction current is delivered by tube P_{vc}. T_{vc} is a centre-tapped transformer. The remaining letters have the same meaning as in fig. 11.

Fig. 14 shows the essentials of a circuit from which the correction current can be obtained. Voltages e_1 and e_2 are sawtooth waveforms of opposite sense and have the frame frequency, $1/T_r$. Switches S_1 and S_2 (in reality they are valves) are closed only during the flyback of the line sawtooth. When they are open, good approximations for the voltages u_1 and u_2 across capacitors C_1 and C_2, are:

$$u_1 \approx (E+e_1)\,\frac{t-nT_l}{RC},$$

$$u_2 \approx (E+e_2)\,\frac{t-nT_l}{RC},$$

where E is a direct voltage, R is the value of the resistors in series with each capacitor (both capacitors have the value C), T_l is the line period, n is an integer indicating the order of the line in the raster ($1 \leqslant n \leqslant 625$ for the 625-line system) and t is an instant such that

$$nT_l < t < (n+1)T_l.$$

If $\hat{e}$ is the peak value of e_1 and e_2, and $\beta = \hat{e}/E$, then

$$E + e_1 = E\left(1 - \beta + \beta\,\frac{t}{T_r}\right)$$

and

$$E + e_2 = E\left(1 - \beta\,\frac{t}{T_r}\right).$$

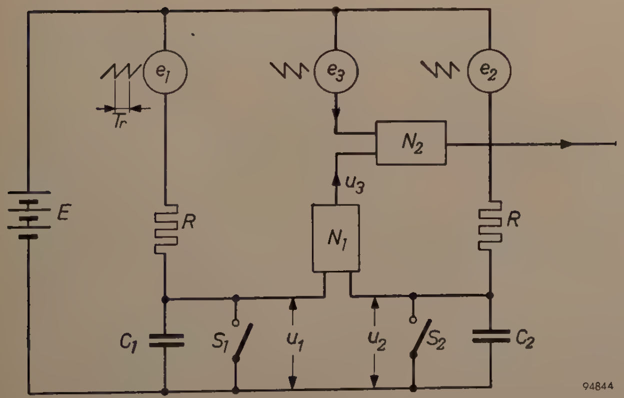

Fig. 14. Schematic diagram of the circuit for generating i_{vc}, the current for correcting trapezium distortion. Switches S_1 and S_2 (in reality they are valves) are closed only during the flyback of the line sawtooth. e_1, e_2 and e_3 are sawtooth voltages having the frame frequency. The subtraction $u_1 - u_2 = u_3$ takes place in network N_1, the addition $u_3 + e_3$ in network N_2.

This gives us the following for the voltages across the capacitors:

$$u_1 \approx E\left(1 - \beta + \beta\,\frac{t}{T_r}\right)\frac{t-nT_l}{RC},$$

$$u_2 \approx E\left(1 - \beta\,\frac{t}{T_r}\right)\frac{t-nT_l}{RC}.$$

These voltages have the waveforms shown in *figs. 15a* and 15*b*, respectively. The difference between the two is a voltage u_3 whose waveform is as shown in fig. 15*c*:

$$u_3 = u_1 - u_2 \approx \beta E\left(-1 + \frac{2t}{T_r}\right)\frac{t-nT_l}{RC}.$$

This needs only the addition of a sawtooth voltage

$$e_3 = \tfrac{1}{2}\beta E\left(1 - \frac{2t}{T_r}\right)\frac{T_l}{RC}$$

at the frame frequency (fig. 15*d*) to give a voltage of the desired shape (fig. 15*e*, cf. fig. 8*a*). The subtraction of u_2 from u_1 takes place in network N_1, the addition of e_3 to u_3 in network N_2.

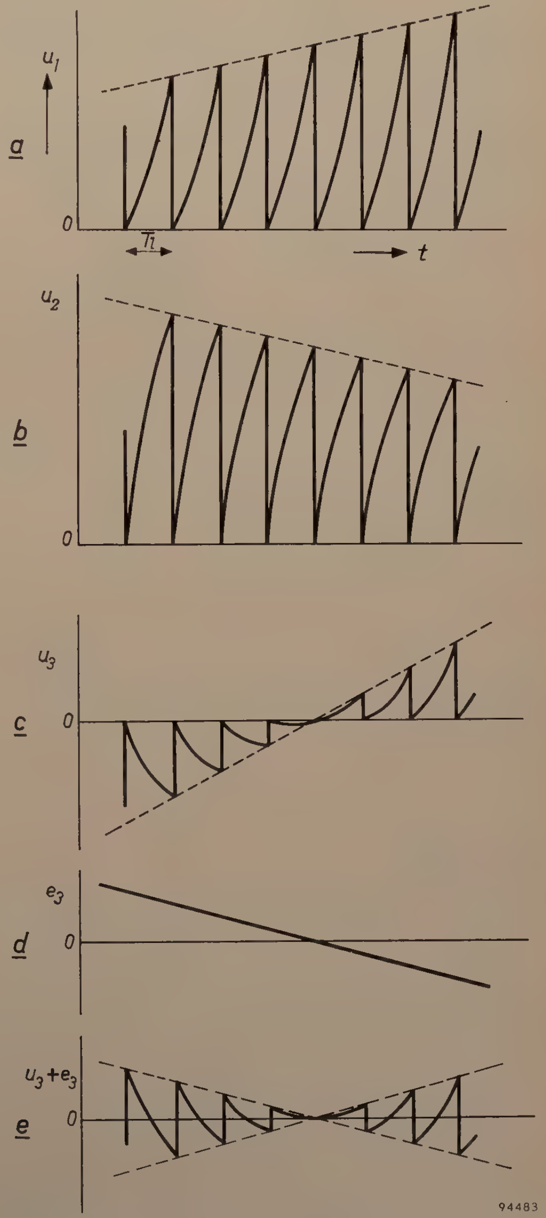

Fig. 15. Voltage waveforms u_1 and u_2, $u_3(= u_1 - u_2)$, e_3 and $u_3 + e_3$ occurring in the circuit of fig. 14.

The *line* scanning currents of the outer CRTs must be corrected in opposite senses by currents such as were indicated in fig. 6*b*. The shape is approximately parabolic. A correction current of this kind can be obtained by introducing a sawtooth voltage $e_{\rm hc}$ of line frequency in series with the scanning coils. Over one line period $e_{\rm hc}$ can be written as

$$e_{\rm h} = A\,t \quad (\text{for } -\tfrac{1}{2}T_{\rm l} \leqq t \leqq +\tfrac{1}{2}T_{\rm l}),$$

A being a factor of proportionality. In the parallel arrangement of coils of inductance L, this voltage produces a current $i_{\rm hc}$ which, if losses can be neglected, may be written as:

$$i_{\rm hc} = \frac{1}{L}\int e_{\rm hc}\,{\rm d}t.$$

Apart from a constant of integration, this is equal to $(A/2L)t^2$ and thus corresponds to a curve of parabolic shape. The circuit is given in *fig. 16*. Like that of fig. 13, it is balanced in such a way as to prevent interaction between the two generators.

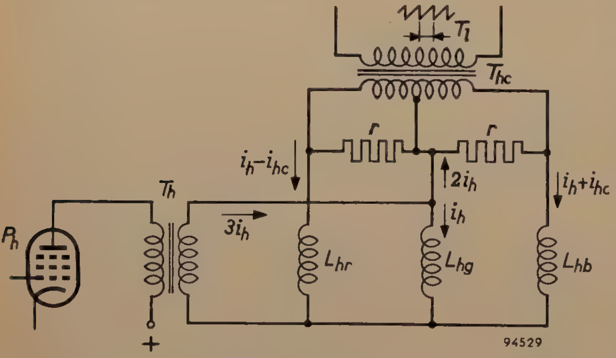

Fig. 16. Circuit for adding correction current $i_{\rm hc}$ to the line scanning current $i_{\rm h}$ in the inductances $L_{\rm hr}$ and $L_{\rm hb}$. Transformer $T_{\rm h}$, supplied from the output tube $P_{\rm h}$, delivers an uncorrected sawtooth current $3i_{\rm h}$. The centre-tapped transformer $T_{\rm hc}$ supplies resistors r with a sawtooth voltage, which causes $i_{\rm hc}$, a correction current of parabolic shape, to flow through inductances $L_{\rm hr}$ and $L_{\rm hb}$.

Displacement and rotational alignment of the images on the projection screen

If the three primary-colour images are to be in exact registration, it must be possible to shift them across the projection screen until their centres coincide, and then to turn them about their common centre until the lines of each raster are exactly horizontal. The latter operation is carried out by turning the deflection coils about the tube axes by means of trimming knobs.

Displacement of the images can be effected in various ways; it can be done with the aid of adjustable direct currents, by turning the focussing coils about axes perpendicular to the axis of the tube, or by altering the alignment of the primary-colour projectors.

1) If an adjustable direct current be passed through each of the six scanning coils, a steady magnetic field of adjustable strength and direction will be set up across each of the CRTs; by this means each electron beam can be biased in direction to the desired degree. The advantage of this method is that the operation can be performed by remote control. But it has a number of disadvantages; one is that the currents have to be stabilized, owing to the temperature dependence of the resistance of the scanning coils.

If the scanning currents are already being subjected to various kinds of correction, there are objections to passing an adjustable direct current through the coils in addition to the others. Separate windings can be incorporated in the coils for carrying these direct currents, but then a high impedance has to be placed in series with the extra windings, since they would otherwise act as short-circuited loops coupled to the scanning windings.

Fitting the direct-current coils in a position before the focussing coils (i.e. nearer the electron gun) is another possibility. Care has to be taken that they do not interfere with the focussing of the beam, and cause part of it to strike the tube diaphragm.

2) It is also possible to give a directional bias of adjustable strength and direction to the electron beam by altering the position of the focussing coil with respect to the axes of the tube. This calls for a mechanical contrivance enabling each of the focussing coils to be turned about two axes at right angles to each other and to the axis of the tube. The method has proved to be very stable and quite satisfactory in practice, in spite of one objection. This arises from slight differences in the position of the electron gun in different projection tubes. For correct superposition of the projected images, it is necessary that the three focussing coils should occupy different positions with respect to the nominal axis of the system. If the "general focussing control" is turned once the projected images have been made to coincide, the three focussing currents will increase or decrease to the same extent, but the images will shift arbitrarily (in directions depending on the position that the gun happens to have in each tube) and superposition will be lost. It is therefore necessary to start by focussing the three images, each of the three focussing currents being separately adjusted, and to adjust for superposition only after this has been done.

The difficulty might be avoided by first setting the focussing coils into a position such that the images would not shift when the value of the focussing current was changed. However, owing to the position of the electron gun, this would generally result in part of the CRT image falling outside the tube screen, which would obviously be quite impermissible. In any case it is desirable that the CRT images should as far as possible occupy the same position on the tube screens, to obviate differences in distortion (due to both optical and electron-optical causes).

3) Altering the alignment of the primary-colour projectors is a purely mechanical operation which can easily be made very stable. For this purpose it must be possible to turn each projector about two axes perpendicular to each other and to the axis of the projector itself. Preferably the two axes should pass through the centre of the corrector plate, but this need not necessarily be the case, if using other axes simplifies the mechanical design. Movement of the projectors about the two axes will then involve a change in their distance from the projection screen, but so small a change that it will not cause any noticeable error.

In the projectors constructed in this laboratory use has been made of a combination of methods (2) and (3); the CRT images are moved into as nearly central a position as possible on the tube screens by turning the focussing coils (i.e. by turning screws *1* and *2*, see fig. 10). The three projected images are then made to coincide on the viewing screen by altering the alignment of the projectors.

Extra-high-tension supply

Our small-screen projection sets are supplied with EHT at 25 kV, the large-screen sets with EHT at 50 kV. It is very important that the EHT supply should be kept strictly constant in spite of fluctuations in the load and in mains voltage. Changes in EHT voltages are accompanied by the following phenomena:

a) A change in the size of the images, due to the fact that the deflection sensitivity depends on the EHT value. Small changes of dimension are permissible providing they affect the three primary-colour images simultaneously and to the same extent. In view of this, the EHT supply for the three projection tubes is provided from a common source.

b) Mutual displacement of the three primary-colour images. The directional bias imposed on the electron beam referred to in the previous section generally differs in amount and direction in the three projection tubes, being dependent on the position that the electron gun happens to have; the consequence is that the three primary-colour images move in different directions when the EHT value changes, superposition thus being lost.

c) Loss of electron-optical focus, resulting in loss of definition.

The EHT value can be rendered more or less independent of the load current by applying parallel stabilization and/or negative feedback.

The term "parallel stabilization" refers to a circuit in which a triode in parallel with the load is controlled in such a way that the total load, consisting of the triode and the three projection tubes, is kept constant. The method is suitable for all systems of generating EHT. Triodes have been developed for this purpose that are capable of standing voltages as high as 80 kV, allowing parallel stabilization to be applied in all cases arising in practice.

Another method makes use of a combination of current and voltage feedback into the EHT generator, which should preferably consist of an oscillator generating a voltage with a fairly high frequency plus a cascade arrangement of diodes and capacitors (voltage multiplier) [6]). A control voltage whose value is dependent both on the load current and on the value of the EHT acts on the oscillator — being applied to its control grid, for example — and on the control curcuit of the regulated HT supply of the oscillator. In this manner it is possible to keep the EHT value constant to within 0.5% over the whole range of load currents.

Neither stabilizing arrangement reacts quickly enough to sudden changes in the load. The circuit should include a buffer capacitor of sufficiently high value to absorb any rapid changes.

The effect of fluctuations in mains voltage can largely be neutralized by using a mains voltage stabilizer or by electronic stabilization of the oscillator HT supply.

Proportional brightness control

It is desirable that a colour-television projector should have facilities for adjusting background brightness by means of a single control. This control, called a proportional brightness control, allows the bias voltages on the control grids of the three CRTs to be altered simultaneously, and in such a way that the colour of the projection screen is always a neutral grey when no video signal is coming in, whatever the position of the control knob. The condition for this may be derived as follows.

---

[6]) J. J. P. Valeton, Philips tech. Rev. 14, 21-32, 1952/53.

The luminous flux Φ emitted by a cathode ray tube is related to the grid voltage (measured from the cut-off value) by the following approximate expression:

$$\Phi = c\, V^{\gamma}, \qquad \ldots\ldots\ (9)$$

where c is a constant and the exponent γ has a value between 2 and 2.5. The condition for obtaining standard white C on the projection screen, from a mixture of the primary colours employed, is that

$$\Phi_{\rm r} : \Phi_{\rm g} : \Phi_{\rm b} = 29 : 51 : 20.$$

The voltages on the three control grids must therefore be in the following proportions:

$$V_{\rm r} : V_{\rm g} : V_{\rm b} = \left(\frac{29}{c_{\rm r}}\right)^{1/\gamma} : \left(\frac{51}{c_{\rm g}}\right)^{1/\gamma} : \left(\frac{20}{c_{\rm b}}\right)^{1/\gamma}, \quad (10)$$

$c_{\rm r}$, $c_{\rm g}$ and $c_{\rm b}$ being values of the constant c in (9), appropriate to the red, green and blue tubes respectively. Since the proportions on the right-hand side of (10) are independent of brightness, it must be possible to achieve the aim in view with linear variable resistors.

The circuit employed is shown in *fig. 17*. The brightness of the red, green and blue tubes is adjusted separately by means of control knobs $2_{\rm r}$, $2_{\rm g}$ and $2_{\rm b}$, Each knob actuates two variable resistors ($R_{\rm r}'$ and $R_{\rm r}''$, $R_{\rm g}'$ and $R_{\rm g}''$, $R_{\rm b}'$ and $R_{\rm b}''$) ganged in such a way that their total resistance always remains constant; hence the voltage across potentiometers $P_{\rm r}$, $P_{\rm g}$ and $P_{\rm b}$ is independent of the position of controls $2_{\rm r}$, $2_{\rm g}$ and $2_{\rm b}$. Potentiometers $p_{\rm r}$, $p_{\rm g}$ and $p_{\rm b}$ are the proportionality controls; they select the fraction of the voltage at the sliders of $P_{\rm r}$, $P_{\rm g}$ and $P_{\rm b}$ (ganged, and adjusted by knob *1*) that is applied to the grids of the projection tubes. Once $2_{\rm r}$, $2_{\rm g}$ and $2_{\rm b}$, and $p_{\rm r}$, $p_{\rm g}$ and $p_{\rm b}$, have been correctly set, the background brightness can be adjusted by turning knob *1*, without any change in the neutral tint on the projection screen. The circuit has the attractive characteristic that, when knob *1* is in the zero position, the right settings of $2_{\rm r}$, $2_{\rm g}$ and $2_{\rm b}$ can be found irrespective of the settings of $p_{\rm r}$, $p_{\rm g}$ and $p_{\rm b}$. If this were not so, finding the right settings of knobs *2* and knobs p would involve repeated adjustment of first the one set and then the other.

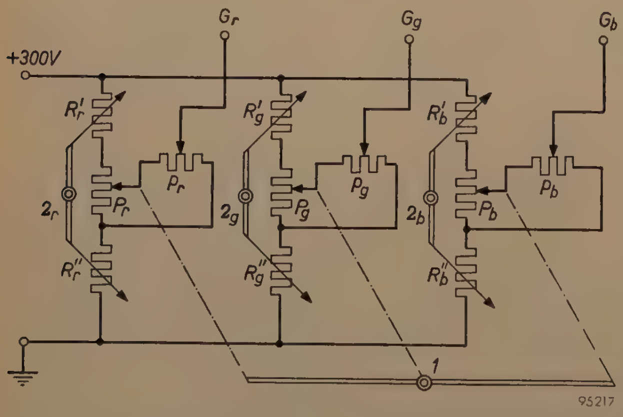

Fig. 17. Schematic diagram of the proportional brightness control. Bias voltages for the red, green and blue CRTs are derived from points $G_{\rm r}$, $G_{\rm g}$ and $G_{\rm b}$. *1* is the knob for adjusting general brightness level via the ganged potentiometers $P_{\rm r}$, $P_{\rm g}$ and $P_{\rm b}$. $2_{\rm r}$, $2_{\rm g}$ and $2_{\rm b}$ are knobs for adjusting the brightness of the red, green and blue images separately. The potentiometers $p_{\rm r}$, $p_{\rm g}$ and $p_{\rm b}$ are for obtaining the right proportions between the brightness values of the three images.

It may be said that the separate brightness controls *2* serve to compensate differences in the cut-off voltages of the projection tubes and that the proportionality controls p serve to compensate differences in slope. In reality the projection tubes do not obey law (9) exactly; however, since it is generally only necessary to adjust background brightness over a small range, departures from the correct colour balance are only very slight.

The video amplifiers

Each of the three projection tubes has its own video amplifier. Besides performing all that is normally required of a video amplifier, the three amplifiers must satisfy special requirements arising from the fact that they are together responsible for the colour rendering of the picture on the projection screen.

In colour television systems, as in black-and-white systems, measures are taken at the transmitter to compensate non-linearity in the receiver picture tube (as exemplified by eq. (9) [7]). In theory, therefore, the receiver video amplifiers should be completely linear, so that the overall channel (camera to projection screen) will be linear, as it must be if colours are to be reproduced correctly. If the three amplifiers are fed with the same video signal, the amplitudes at the three inputs being in certain proportions, a monochrome image must necessarily appear on the screen. However, if the characteristics of the projection tubes differ from the nominal characteristic on which the compensation at the transmitter is based, the range of greys between black and white will no longer be faithfully reproduced. It will in fact contain regions that, instead of being neutral in tone, will exhibit a tint that depends on the differences between the actual and the nominal characteristics of the CRTs. What is more, few of the other colours will be faithfully reproduced.

---

[7] See the concluding observations in article I (footnote [1]).

As we have seen earlier, to get a given grey shade on the viewing screen, it is necessary that the quantities of red, green and blue light should be present in a certain specific proportion. Because the characteristics of the CRTs conform to the law $\Phi = cV^{\gamma}$, the control voltages will again be in specific — although different — proportions. But in practice the light flux from a CRT screen does not obey the law exactly, one of the main causes being the saturation of the phosphors. There are differences in the properties of the three phosphors; moreover, the anode currents of the CRTs are not equal when adjusted to produce a grey shade on the projection screen. In consequence, deviations from the law $\Phi = cV^{\gamma}$ are not the same for the three primary colours, being greatest for the red phosphor which exhibits the greatest degree of saturation. The saturation effect is particularly strong in apparatus for large-screen projection, which involves a high specific loading of the phosphors. In practice the control voltages on the three CRTs are adjusted to values such that grey shades are properly reproduced in both the lighter and darker parts of the picture (*fig. 18*); the values chosen for the bias voltages are such that the tubes are just cut off when no signal is coming in. It will be seen from fig. 18 that the proportion of red light on the projection screen is too great throughout the range of greys between black and brightest white. This effect can be compensated by introducing non-linearities into the video amplifiers such that amplification is higher in the darker parts of the picture than it is in the

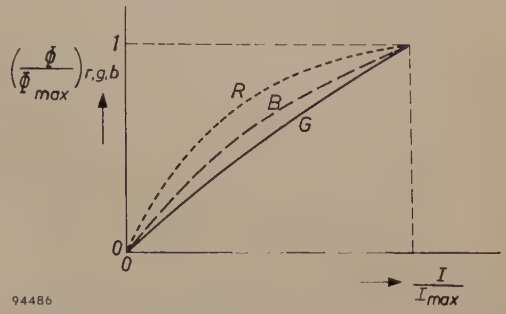

Fig. 18. Ratio of the luminous flux Φ to $\Phi_{\max}$ as a function of the ratio of anode current I to $I_{\max}$, for the red, green and blue projection tubes (R, G and B respectively). Saturation is heaviest in the red CRT and lightest in the green one.

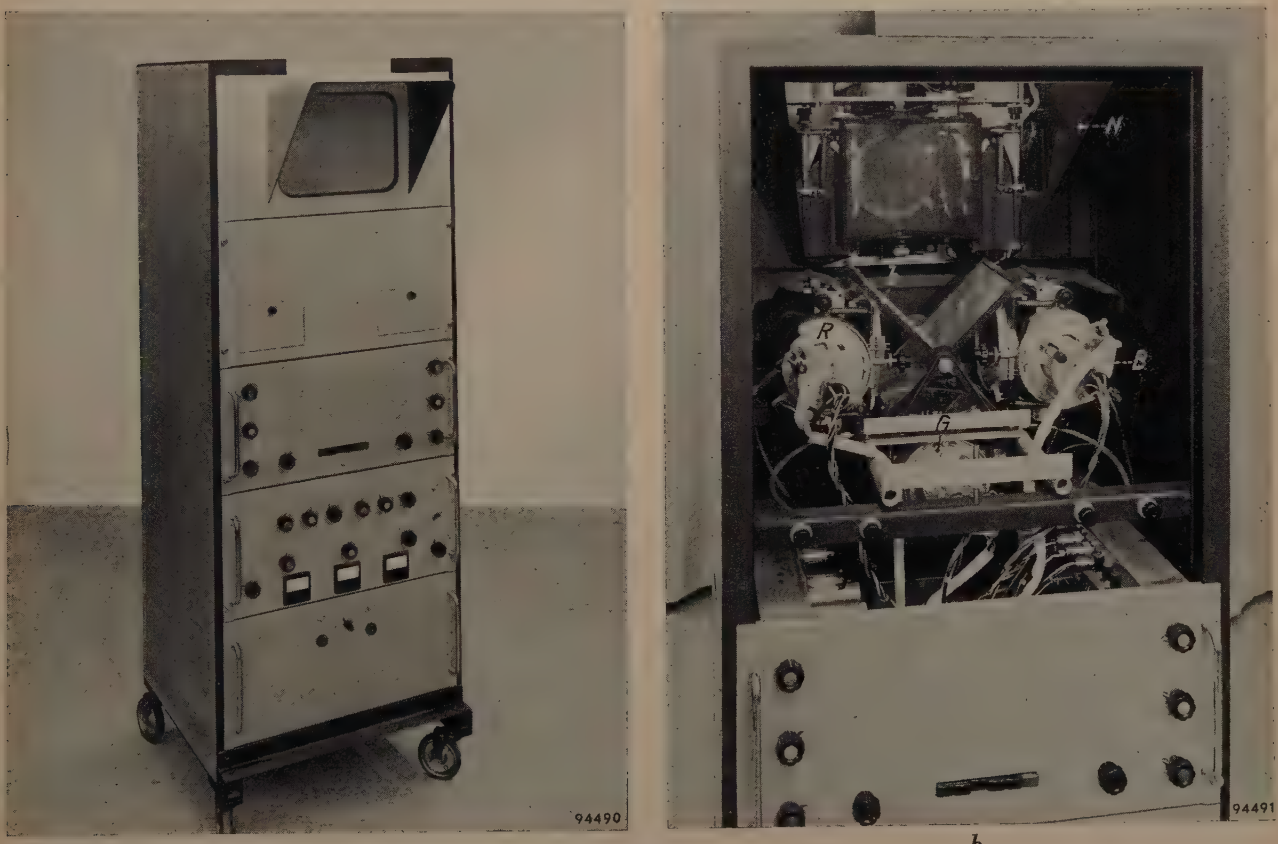

a *b*

Fig. 19. Colour television projection set for studio monitoring (picture size 22 cm × 29 cm, maximum luminance 200 cd/m²). *a*) The complete set, with transmission projection screen of polyvinyl chloride. *b*) View of the set with the two upper panels removed; *R*, *G* and *B* are the primary-colour projectors, which are on the folded-beam principle. *r* and *b* are the crossed dichroic mirrors. *N* is a plane mirror inclined at 45°.

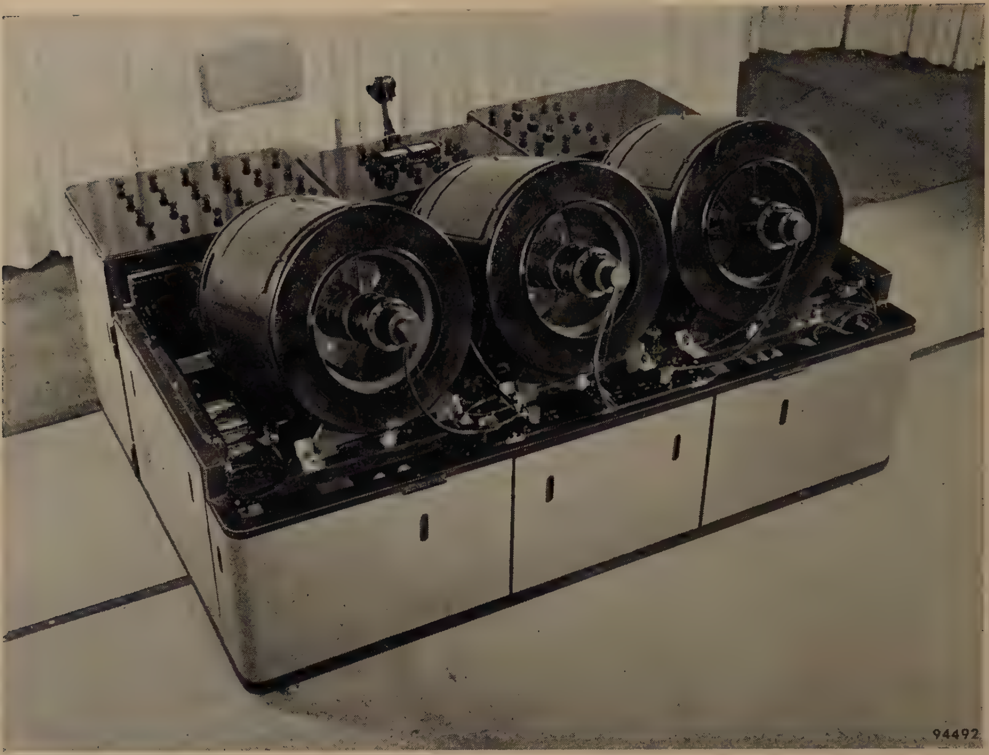

Fig. 20. Large-picture projection set with cover removed. The Schmidt optical systems, which are of the "in-line" type, are mounted side by side. See also figs. 21 and 22.

lighter. This implies a voltage characteristic that can often be approximated by two straight lines of different slope [8]).

In addition, the amount of amplification given by the three amplifiers must remain as nearly constant as possible and be independent of the properties of the electronic tubes with which they are equipped. For this to be so, it is often necessary to apply negative feedback and to stabilize the heater current.

Of course, each amplifier must be provided with a contrast control with which the amplification can be adjusted in order to achieve correct colour reproduction.

The projectors constructed

Many of the principles dealt with above have been applied in a number of colour television projectors built in the Philips Eindhoven Laboratory.

In projectors giving relatively small pictures (35 cm × 46 cm and 22 cm × 29 cm) use is made of experimental projection tubes having the same

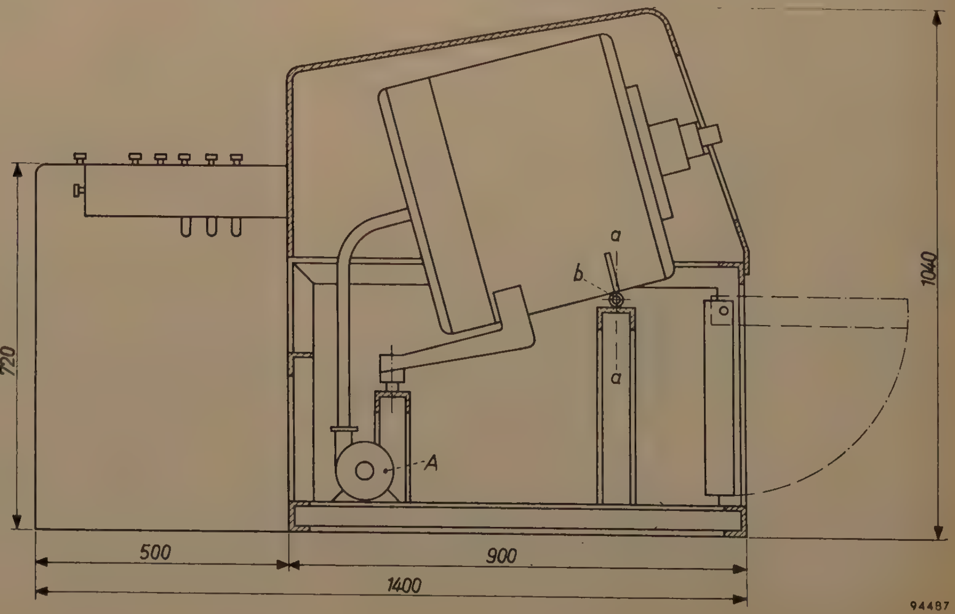

Fig. 21. Sketch showing the principal dimensions of the large-screen projector shown in figs. 20 and 22. Controls within the operator's reach allow him to turn the primary-colour projectors about a vertical axis *a*-*a* (in a ball and socket joint) and about a horizontal axis *b* (perpendicular to the plane of the drawing). *A* is the fan for cooling the projection tubes.

---

[8]) F. H. J. van der Poel and J. J. P. Valeton, Philips tech. Rev. **15**, 221-232, 1953/54.

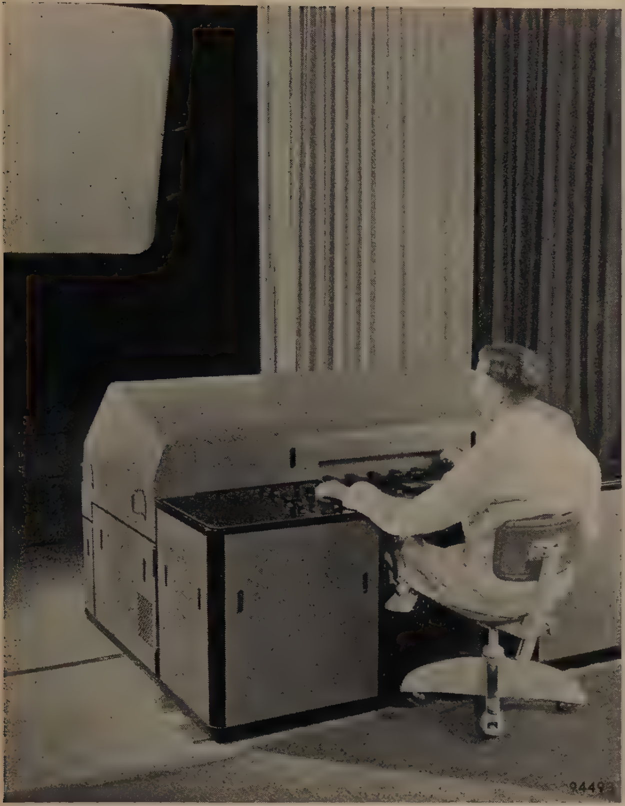

Fig. 22. The projector of fig. 20 in its housing. The picture size is 2.25 m × 3 m ($\approx 7\frac{1}{2}' \times 10'$) and the maximum luminance 20 cd/m^2.

dimensions and supplied with the same voltages as the MW 6-2 monochrome tube [9]) (screen diameter 6 cm, anode voltage 25 kV). Each tube is mounted in a Schmidt optical system with a mirror at 45°, a system of the type originally developed for the MW 6-2 [2]). The light passes through crossed dichroic mirrors, is reflected by a further plane mirror inclined at 45° and falls on to a transmission projection screen of polyvinyl chloride. Grooves on the front and back of the screen give it the desired directional characteristic. *Fig. 19* shows a projection apparatus of this kind, intended for studio monitoring purposes. The picture measures 22 cm × 29 cm and has a maximum luminance of about 200 cd/m^2.

In equipment for large pictures (2.25 m × 3 m) use is made of experimental projection tubes with a screen of 13 cm diameter and an anode voltage of 50 kV. A photograph of a large-screen projection apparatus equipped with these tubes and with dichroic mirrors has been shown in fig. 4, earlier in this article. A maximum luminance of about 10 cd/m^2 is obtained on a beaded screen giving a "gain" of $\mu = 2.8$. Electrical adjustments are made by remote control, from a desk at the rear of the hall.

In another type of large-screen projector use is made of "in-line" Schmidt optical systems mounted side by side (*figs 20* and *21*). In this apparatus the control panel forms an integral part of the projector unit (*fig. 22*). Amongst the controls on the panel are six knobs for altering the alignment of the primary-colour projectors. These can be turned about two axes, a vertical axis *a-a* (fig. 21) and a horizontal axis through the points *b*. The apparatus embodies neither dichroic mirrors nor 45°-mirrors, giving as a result a maximum luminance of about 20 cd/m^2 on the screen (again a beaded screen with a μ of 2.8). Moreover, definition and contrast are considerably better in this projector than in that of fig. 4, and its height (fig. 21) is a good 30 cm less.

Summary: In the reproduction of colour television pictures by projection methods, three cathode-ray tubes of the projection type are used having respectively red, green and blue fluorescing phosphors. Each tube is mounted in a Schmidt optical system, either of the "in-line" type or of the "folded" type. The article is largely devoted to discussing two methods of obtaining superposition of the three primary-colour images. In the first method dichroic mirrors are employed in combination with folded optical systems. All three images are virtually projected from a single point; in theory, therefore, they are superimposed from the outset. This is not the case in the method where the primary-colour projectors are mounted side by side, but not parallel to one another; here the two outside tubes project images of trapezium shape. The trapezia can be converted into rectangles by making certain modifications to the scanning currents of the outer tubes. The current waveforms required for trapezium correction are discussed, as also the manner of generating them. Other matters dealt with in connection with scanning are skew correction, the adjustment of amplitude, and the displacement and rotational alignment of the images on the projection screen. Extra high tension stabilization methods, proportional brightness control and the characteristics of the video amplifiers are also discussed. Finally, some details are given of a number of colour television projectors actually constructed in the Philips laboratory at Eindhoven. Of two studio monitoring sets whose optical systems embody dichroic mirrors, one projects a picture measuring 22 cm × 29 cm, the other a picture measuring 35 cm × 46 cm; the maximum luminance is 200 cd/m^2. One large-screen projection set embodying dichroic mirrors gives a picture 2.25 m × 3 m with a maximum luminance of 10 cd/m^2; another, in which the primary-colour projectors are mounted side by side, gives a picture 2.25 m × 3 m with a maximum luminance of 20 cd/m^2.

---

[9]) J. de Gier, Philips tech. Rev. **10**, 97-104, 1948/49.

THE PHILIPS PAVILION AT THE BRUSSELS WORLD EXHIBITION

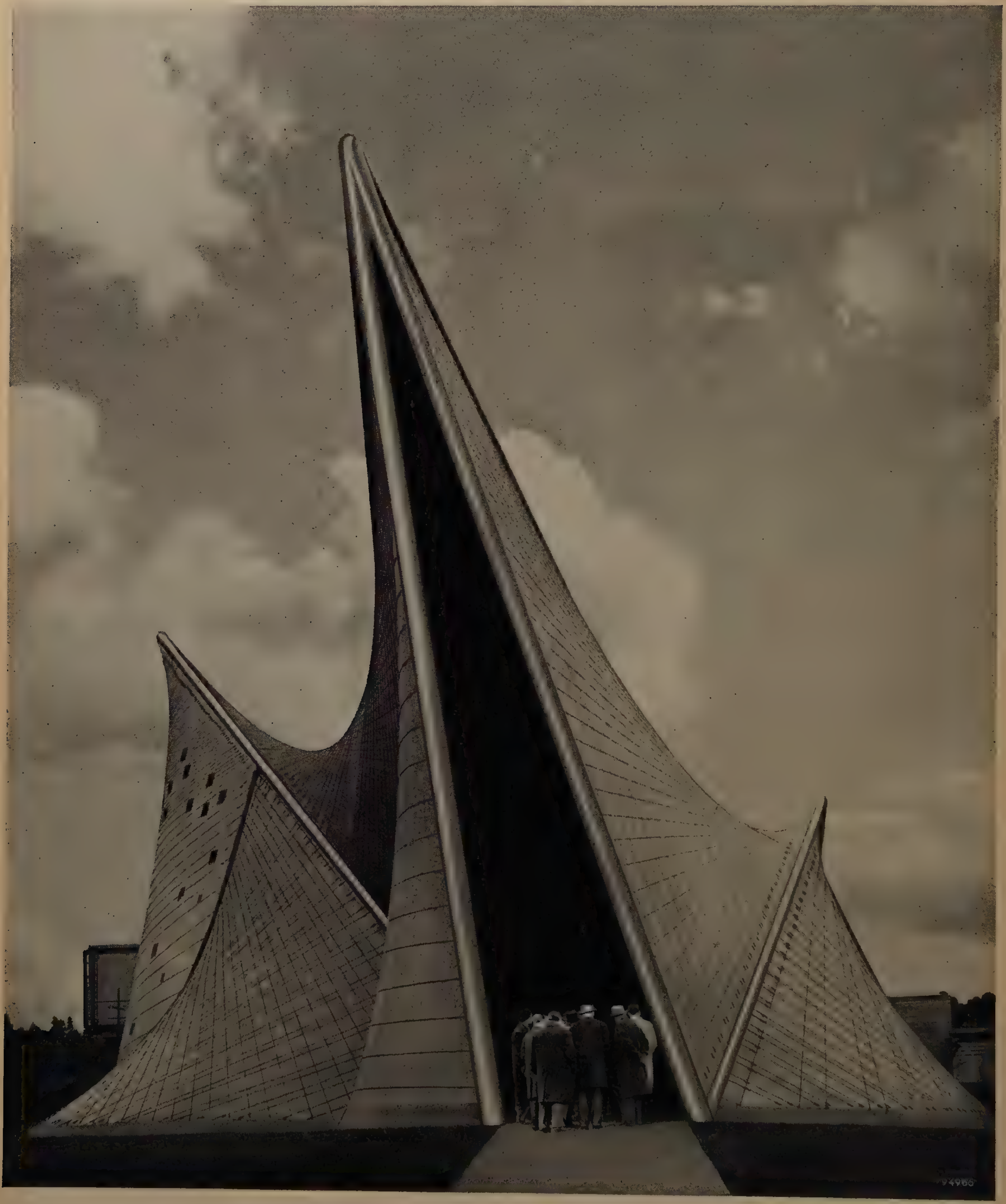

In this building, designed for Philips by the architect Le Corbusier and his collaborator Y. Xenakis, an "Electronic Poem" is performed for visitors to the Brussels Exhibition. It is a composition of light and sound, the scenario being by Le Corbusier and the Music by Edgar Varèse. The unusual but effective architectural conception of the building and its construction in prestressed concrete will be the subject of a number of articles in one of the following issues of this Review. It is also the intention to publish a subsequent article on the technical aspects of the "Electronic Poem".

THE GENERATION OF DISLOCATIONS BY THERMAL STRESSES

by P. PENNING.

548.4:546.289

The term dislocation, denoting a particular kind of lattice imperfection in crystalline materials, was first introduced about 20 years ago. Since then dislocations have ~~lost~~ their hypothetical status — their existence is now well-established and they play an essential role in the behaviour of crystalline solids.

Dislocations (and other lattice imperfections) have a marked influence on the physical and mechanical properties of solids. This is of particular interest in the semiconducting materials germanium and silicon, which are nowadays of considerable technical importance. It is therefore not surprising that dislocations and their properties are the subject of a great deal of research. The present article deals with the formation of dislocations during the cooling of a germanium crystal, the study of which is important both with regard the problem of how to control the properties of germanium more effectively, and in order to throw fresh light on the origin of dislocations.

The preparation of single crystals of germanium

The importance of the elementary semiconductor materials germanium and silicon for various electronic devices is well known. Before these materials can be put to practical use, however, for example in the manufacture of transistors, they must be prepared in the form of single crystals of well-defined composition. This is generally done by causing the molten material to solidify under carefully controlled conditions. Of the various methods that have been developed we shall briefly describe here the Czochralski method, and confine ourselves mainly to the material germanium, though much of what will be said is also applicable to other methods and to silicon.

In the Czochralski method a seed crystal, mounted at any desired orientation, is lowered into a crucible containing molten germanium. If the temperature of the molten germanium is only slightly above the melting point, the seed, when pulled slowly upwards, will begin to grow and a single-crystal of cylindrical shape is formed. As the crystal is pulled out of the melt the solidified material cools off. Since in general the dimensions of the withdrawn crystal rod are fairly large (generally one or more cm thick) the inner material cools down more slowly than the material at the surface. This gives rise to temperature differences between axis and periphery, the magnitude of which are determined by the size of the crystal rod, the thermal conductivity of the crystal, the rate of withdrawal, the constitution of the gas ambient in which the growth takes place, etc.

The greatest temperature differences will generally occur immediately above the plane of solidification and may amount to as much as 40 °C. As a result of the thermal expansion, the central regions, being at a higher temperature will try to expand. This, however, is opposed by the surrounding material. The consequence is a fairly complex state of deformation, which can best be described by considering the stresses accompanying the process (forces between warmer and colder parts).

Such thermal stresses are of course present not only during the cooling of the material from the melt; they will always be present when a material is unevenly heated or cooled. Apart from the obvious case of a uniform temperature distribution, there is only one non-uniform temperature distribution which can be shown to give rise to no internal stresses, namely that at which the temperature *gradient* in the material is the same everywhere.

The thermal stresses are accompanied in the first place by an elastic, reversible deformation; as soon as the temperature again becomes uniform the deformation disappears. If the thermal stress is large, two subsidiary, permanent effects may appear. Firstly, if the material is brittle it may fracture. An example will be given below. Secondly, if the material is ductile it may be plastically deformed. This deformation is associated with the occurrence of lattice imperfections, such as dislocations, vacancies, etc. ¹), and hence destroys to some extent the perfection of the single crystal. How large the plastic deformation is, compared with the elastic deformation, depends entirely on the properties of the material and on the magnitude of the stress. Since the introduction of lattice imperfections generally has an adverse effect on the material, the aim during growth and all other treatments to

---

¹) For a discussion of the mechanism of the plastic deformation of crystals, see, for example, H. G. van Bueren, Lattice imperfections and plastic deformation in metals, Philips tech. Rev. **15**, 246-257 and 286-295, 1953/54.

which the crystal is subjected is to keep the thermal stresses as small as possible. To avoid them entirely is not possible in practice.

As regards one kind of lattice imperfection viz. dislocations, it is fortunate that in a number of cases, including that of germanium, they can be made visible. When a polished germanium surface is etched with a special agent, almost every dislocation terminating at the surface gives rise to an etch pit (*fig. 1*). These etch pits can be counted and their distribution over the surface studied. This makes it possible not only to discover the concentration of these imperfections but also to investigate the conditions under which they arise, and hence to modify these conditions for the better.

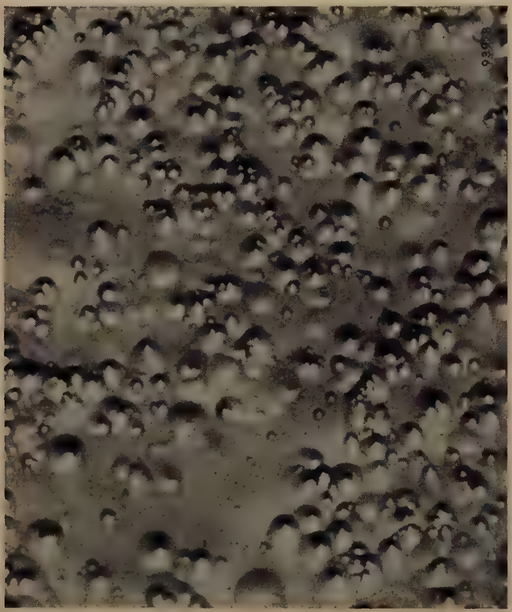

Fig. 1. Etch pits on the surface of a slightly deformed germanium crystal. The pits indicate the places where dislocation lines terminate at the surface (magnification 75×).

In the following we shall first consider the thermal stresses produced in germanium during certain experiments, and their effects on the etch-pit pattern. After a digression into the theory of the plastic deformation of germanium, we shall examine the information to be derived on the nature of this deformation from the observations described.

Thermal stresses in germanium rods during cooling

As will be clear from the foregoing, during the cooling of a hot cylindrical rod the cooler outermost parts of the rod will try to shrink more than the average and the warmer innermost parts less. As a result, the outermost parts will be subject to a tensile stress and the innermost parts to a compressive stress.

If the cylinder is cooled very rapidly (quenched), for example by plunging it into a bath of much lower temperature and good heat conductivity, stresses will *initially* be set up only at the surface, but these will be very large indeed. We can estimate these stresses as follows. Assume that, immediately after quenching, the mass of the material is still entirely at the initial high temperature T_0, but that the surface has taken on the quench temperature T_f. A very thin layer at the surface will then try to shrink by the relative amount $\varepsilon = \alpha(T_0 - T_f)$ where α is the coefficient of thermal expansion. It is prevented from doing so by the underlying material, and thermal stresses are set up (in this layer alone) which oppose the shrinkage. Since there are no external forces acting on the crystal, these can only be tangential (suffix t) and axial (suffix z) stresses in the surface layer.

From the theory of elasticity we know that these stresses amount to

$$\sigma_t = \sigma_z = \frac{E}{1-\nu}\,\alpha(T_0 - T_f)\,, \qquad (1)$$

in which E is Young's modulus and ν is Poisson's ratio. According to this formula, immediately after the quenching of a germanium crystal over several hundreds of degrees, stresses will be set up in the surface layer amounting to some tens of kg/mm². These can easily exceed the critical stress for cleavage, which for germanium is about 20 kg/mm². Hence surface cracks will appear in the germanium rod, which accommodate the thermal stresses to such an extent that elsewhere in the rod no appreciablic plastic deformation occurs. This was confirmed by the following experiment. A germanium rod at a temperature of 500 °C was suddenly plunged into a water bath. Theoretically, according to (1), this would produce stresses of approximately 50 kg/mm² After the experiment the rod showed a large number of surface cracks (*fig. 2*); examination under the microscope revealed that, to judge from the number

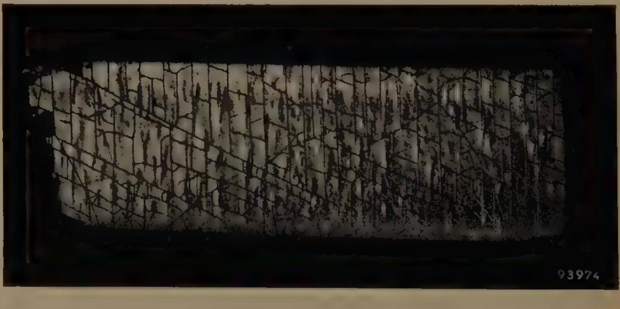

Fig. 2. Surface of a germanium rod quenched from 500 °C in a water bath. The crystal becomes covered with a large number of surface cracks (actual size).

of etch pits, no significant increase in dislocation density had taken place between the cracks.

Entirely different results are found if a germanium crystal is cooled relatively slowly, for example in a stream of gas. The whole process now takes place much less abruptly: the heat flux (which, in a long cylinder, is mainly radial) is much smaller, and in order to evaluate the maximum stress we must take time effects into account. Following the classical methods of solving heat-conduction problems, we can plot the deformations tending to arise from temperature differences as a function of time and place, provided the heat flux at the surface is known. The thermal stresses can then be ascertained with the aid of elasticity theory. One again finds [2]) that in the very first moments the stresses occur principally in the outermost surface layer, but fairly soon afterwards, before they have reached their maximum value there, stresses begin to arise also in the innermost parts. It appears that when the maximum value is reached at the surface the stresses in the centre are also fairly near maximum. This stress pattern builds up so quickly that the average temperature has dropped only very little by the time the stresses have reached their maximum value. From that point onwards the stresses everywhere start decreasing almost exponentially with time, but there is no further change in the *relative* magnitude of the stresses, i.e. the stress pattern then existing remains as it is, only the absolute values decreasing. The rate of this decrease may be expressed in terms of a characteristic time which is proportional to the radius of the rod, and to the specific heat per unit volume, and inversely proportional to the thermal conductivity of the material. This characteristic time varies between a few seconds and a few tens of seconds in the cases considered here.

The stress distribution set up after the initial period is parabolic across the diameter of the rod and is represented by the following equations (using polar coordinates r, Θ, z)

$$\left.\begin{aligned} \sigma_r &= \left(\frac{r^2}{R^2} - 1\right)\sigma_0, \\ \sigma_\Theta &= \left(3\frac{r^2}{R^2} - 1\right)\sigma_0, \\ \sigma_z &= \left(4\frac{r^2}{R^2} - 2\right)\sigma_0, \end{aligned}\right\} \quad \ldots\ldots \quad (2)$$

where R is the radius of the crystal rod and σ_0 is a term giving the exponential decrease of the stresses with time. The value of σ_0 is given by an expression of the form (1), modified by a factor β which depends on the cooling rate and the dimensions of the rod ($\beta \approx 0.01$ in the tests described below).

Now for the occurrence of plastic deformation — and hence the introduction of lattice imperfections — only the shear stresses acting on certain crystallographic systems are of importance (see [1]) and below, next heading) since a purely hydrostatic pressure (equal compression from all directions) does not give rise to plastic deformation. We may therefore, for convenience, subtract any hydrostatic pressure from equations (2) without affecting the problem. We choose to subtract a pressure equal to σ_Θ, since this enables us to dispose of the second of equations (2). We are left with only two normal stress components, σ_r in the radial direction and σ_z in the axial direction:

$$\sigma_r = -2\frac{r^2}{R^2}\sigma_0, \quad \ldots\ldots \quad (3)$$

$$\sigma_z = \left(\frac{r^2}{R^2} - 1\right)\sigma_0. \quad \ldots\ldots \quad (4)$$

These stresses are both compressive: the radial compression is greatest at the surface and zero at the axis while the axial compression is maximum along the axis and zero at the surface. The maximum values of σ_r and σ_z are $2\sigma_0$ and σ_0 respectively. The value of the factor β being about 0.01, the maximum stress was smaller by approximately this factor than the value 50 kg/mm^2 calculated for rapid quenching, and amounted to a few kg/mm^2. This is of the order of the yield point of germanium at temperatures of about 500 °C. In these circumstances we may expect that at least a part of the thermal stress will be eliminated by plastic flow, and dislocations will be formed.

The following experiments demonstrated that this in fact took place. Germanium crystals of rod-shape, with their axes in a known crystallographic orientation, were heated to 850 °C and then cooled ("quenched") in a stream of hydrogen. Microscopic examination, after etching of a cross-section perpendicular or oblique to the axis of the rod, showed the presence of a typical regular pattern of etch pits, examples of which can be seen in *Fig. 3a* and *b*. The etch pits lie on rows whose direction is found to coincide with the intersections of (111) planes (octahedral planes) with the etched surface [3]).

---

[2]) P. Penning, Generation of imperfections in germanium crystals by thermal strain, Philips Res. Repts. **13**, 79-97, 1958 (No. 1).

[3]) In this article no distinction is made between the symbols (*hkl*) and {*hkl*}, which denote respectively a single plane and the whole family of crystallographically equivalent planes. Nor is any distinction made between the symbols [*hkl*] and <*hkl*>, which refer in a similar way to crystallographic directions.

Which of the four possible (111) planes are involved at any particular region depends on the position of that region in the cross-section.

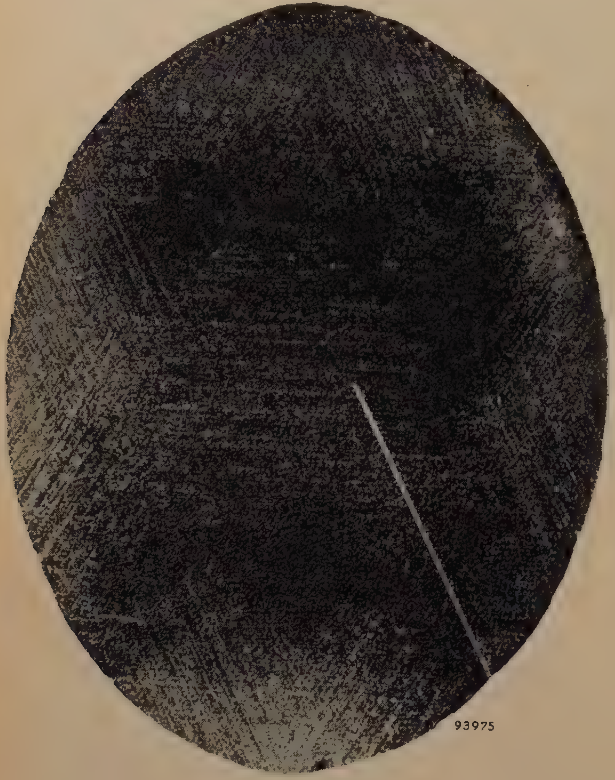

a

b

Fig. 3. *a*) Etch-pit pattern produced after etching on an oblique (111) cross-section of a cylindrical crystal with its axis in a [110] direction, which was cooled in a stream of gas. The etch pits lie in rows parallel to the intersections of the surface with the three other (111) planes. Note the minimum in the etch-pit density about midway along the radius of the cross-section. *b*) Etch-pit pattern for a perpendicular (100) cross-section of a [100] crystal, cooled as (*a*).

The average number of etch pits per cm^2 is hundreds of times larger than it was before heating to 850 °C and cooling; the number is largest at the periphery and smallest in a zone roughly half way along the radius of the cross-section.

These striking aspects of the distribution of the etch pits indicate that the dislocations do indeed arise during plastic deformation due to thermal stresses resulting from cooling.

In order to give a better foundation for this conclusion we shall devote a few words to the mechanism of the plastic deformation of germanium.

Plastic derformation of germanium

Germanium is extremely brittle at room temperature. Under sufficient stress it usually breaks as a result of cleavage along (111) planes, like diamond, to which it is structurally related. It has recently been found that at temperatures above about 400 °C germanium begins to exhibit a certain degree of ductility when the material is subjected to stresses of a few kg/mm^2. The higher the temperature at which the stress is applied the better is the germanium able to yield to this stress by plastic deformation until, near the melting point, it is very ductile. An interesting point is that, where the temperatures are not too high, a certain delay effect is observed: plastic deformation of the germanium occurs only some time after the application of the stress. For example at 400 °C, after application of stress, there may be an incubation period of several minutes before a noticeable deformation begins to take place, and even then it shows the typical character of creep, i.e. it increases only gradually with time. At higher temperatures the delay time decreases very rapidly, and above about 600 °C it is practically no longer perceptible, the deformation taking place almost immediately after the stress is applied.

Microscopic examination of a surface polished beforehand reveals that the mechanism of plastic deformation in germanium is principally a slip mechanism. Slip lines become visible, as shown in *fig. 4*. These slip lines are found to be oriented along intersections with (111) planes and the direction of slip always coincides with a [110] direction. This points very clearly to a dislocation mechanism as observed in metals ^{1}): slip in germanium evidently takes place owing to the formation and movement of dislocations with Burgers vectors along [110] directions over slip planes which have (111) orientations.

The germanium lattice has the same structure as that of diamond. *Fig. 5* shows the elementary cell of the diamond lattice. It will be clear that the (111)

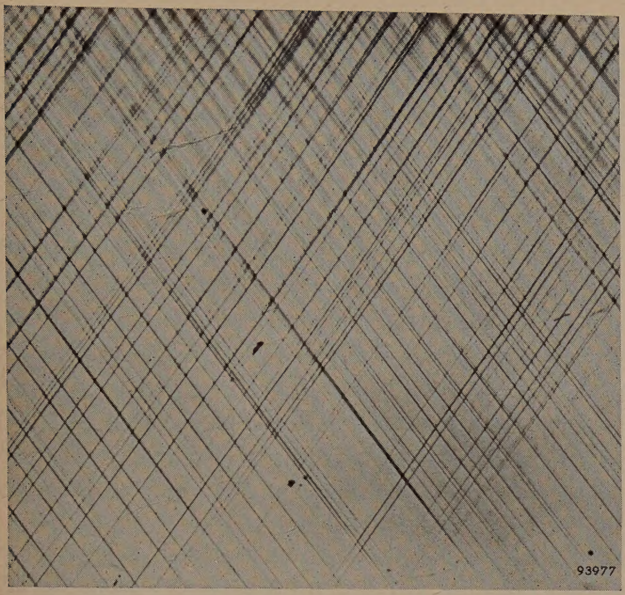

Fig. 4. Slip lines on a (110) plane of a plastically bent germanium crystal (75×). The lines run parallel to (111) planes.

planes are planes of closest packing, and moreover, that the shortest lattice period will be encountered in the [110] directions. On this basis one can understand theoretically the reason for the observed dislocation behavior: the dislocations occurring are those having the lowest energy.

It is to be expected that the density of the dislocations appearing at the surface is greatest in the slip lines. By suitably etching a surface covered with slip lines we will thus obtain rows of etch pits, again running along intersections of the (111) planes with the surface. This is illustrated in *fig. 6*. On the etched face, which is (100), two mutually perpendicular systems of rows of etch pits are visible, corresponding to two sets of (111) slip planes.

The formation and movement of dislocations on a particular slip system — i.e. combination of slip plane and slip direction (Burgers vector) — will occur only providing the shear stress component in the direction of the Burgers vector of this system exceeds a certain critical value. For a given state of stress, this condition will, generally speaking, be satisfied only on a few of the twelve possible slip systems in the diamond lattice. For this reason, the state of stress during the cooling of a cylindrical crystal will give rise to slip only on certain of the possible slip systems, depending on the crystallographic orientation of the axis of the rod. After etching, therefore, a quite specific etch-pit pattern may be expected. We shall now inquire into how far the etch-pit patterns observed after slow cooling are in agreement with these considerations.

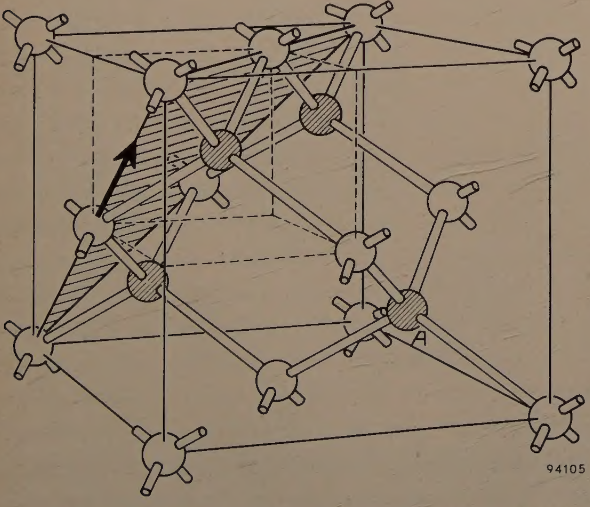

Fig. 5. Unit cell of the diamond structure, the crystalline structure of germanium. The hatching indicates one of the four (111) planes, and the arrow one of the six [110] directions.

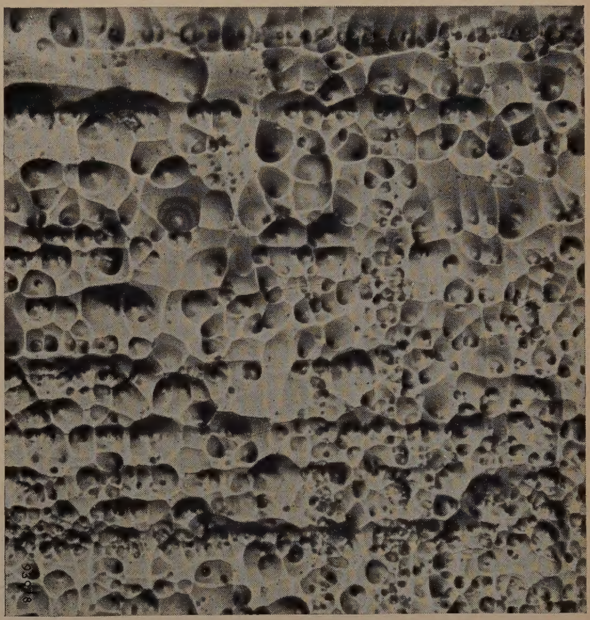

Fig. 6. Etch pits produced after etching a (100) plane, containing slip lines, of a plastically bent germanium crystal. The rows of pits lie along the intersections with (111) planes i.e. along [110] directions.

Distribution of dislocations after deformation by thermal stresses

We have seen that, if the deformations can be regarded as purely elastic, the stress distribution can be approximately given by (3) and (4), at the moment that the stresses are at maximum. Let us now assume that it is this elastic stress distribution which determines the degree of plastic flow. This implies the assumption that only a small proportion of the stresses is eliminated by plastic deformation, so small that the stress distribution is hardly affected thereby. This assumption is by no means self-evident. In view of the considerable plasticity of germanium at high temperatures, one might expect at first sight that almost all differences in thermal expansion would be accomodated by plastic deformation, and that, after cooling, the material would be approximately free of stresses. In that case, of course, (2) would not apply, these formulae being derived from elasticity theory alone. An entirely different distribution of deformations and displacements would then appear instead of the deformations due to elastic thermal stresses, one reason being that plastic flow is only possible in certain directions. This distribution, too, can be calculated. However, for reasons stated below, we shall first confine ourselves to the distribution due to purely elastic stresses and consider a rod-shaped single crystal with a [110] direction parallel to the axis. Fig. 7 shows schematically the orientation with respect to this axis of the four (111) planes, each of which has three [110] directions — giving the twelve possible slip systems. To define the position of any point in a cross-section perpendicular to the axis, two coordinates will be used, namely the distance r from the centre, and the angle Θ between the direction r and the [100] direction. We can now roughly ascertain in the following way when and on what planes slip will occur.

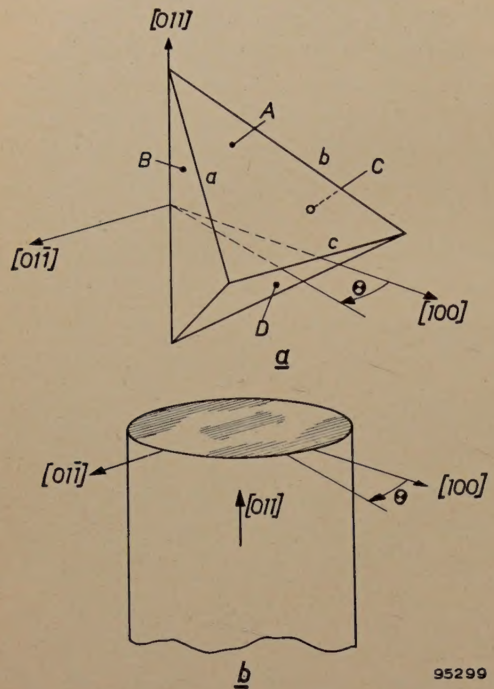

Fig. 7. *a*) The orientation of the four possible (111) slip planes. *A*, *B*, *C* and *D* with respect to the axis of a [011] crystal. The three slip directions in the plane *A* are indicated by *a*, *b* and *c*. *b*) [011] crystal rod cut parallel to (011) plane showing roughly the regions (hatched) where slip on planes *A* takes place (see further fig. 8).

Near the periphery of the rod the radial normal component of stress, σ_r, is predominant. Only where this stress-component makes an angle not too near to 0° or 90°, both with the slip plane and the slip direction, does an appreciable shear stress component act in the slip system concerned, in which case slip may occur. (When a body is acted on by a uniaxial stress σ making an angle φ with the normal to the slip plane and an angle λ with the slip direction, the shear stress component in the slip direction is given by $\tau = \sigma \cos \varphi \cos \lambda$.) Consider the slip plane *A* (*fig. 7a*). This lies favourably for those positions in the cross-section where $\Theta \approx 0°$; here only the slip directions *a* and *b* on plane *A* can be active. For positions corresponding to $\Theta \approx 45°$, the slip direction *c* becomes favourably oriented. For $45° < \Theta < 90°$ the shear-stress component resolved in the plane *A* becomes increasingly smaller, and slip becomes increasingly less probable, until at $\Theta = 90°$ the shear stress acting in this plane has become zero. In the other quadrants the variation with Θ is analogous. In the inner regions, near the axis of the rod, the axial stress σ_z predominates. The probability of slip on plane *A* is there practically independent of Θ. Since, however, the resolved shear stresses due to σ_r and σ_z have opposite sign, the net deformation is zero in those regions where both stresses are of approximately equal magnitude, i.e. about midway along the radius: thus no slip occurs on plane *A* in an annular region (fig. 7*b*). The annular slip-free region is not independent of Θ. At $\Theta = 90°$ and 270° the radial stress component vanishes, as we have seen, so that the outer boundary

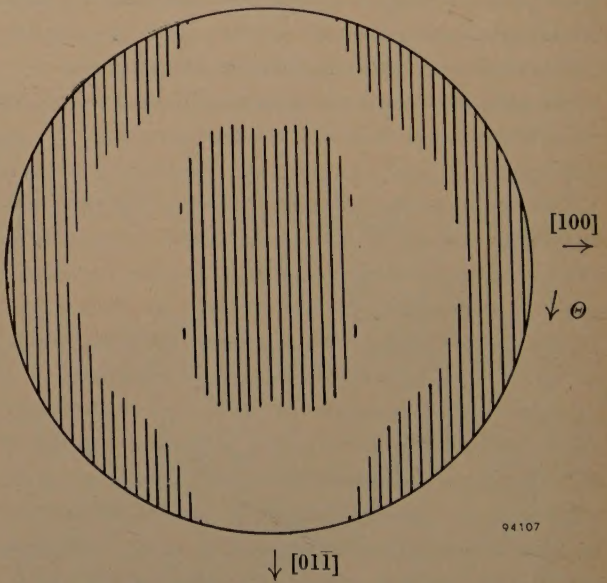

Fig. 8. Cross-section of a[110] crystal showing the regions in which slip on the slip plane *A* (fig. 7) is to be expected due to thermal stresses (i.e. regions where the shear stress in at least one slip direction exceeds a certain value). Between a roughly oval slip zone in the centre and a peripheral zone consisting of two parts, lies a region where there is practically no slip at all.

of the slip-free region extends to the edge of the crystal; also the resolved stress due to the axial component gives rise to slip at points further from the axis in the directions 90° and 270° where the opposing stress due to σ_r is smaller, so that the inner boundary of the slip-free region is roughly oval in shape.

In this way we can indicate roughly in what parts of the cross-section the resolved shear stress will exceed a certain value along at least one of the slip directions of plane A (say), i.e. in what zones slip will take place on plane A, and hence give rise to etch pits at the surface. It should be mentioned that the value chosen for this resolved shear stress is not critical, that is to say, slip patterns of similar form are obtained for a range of values of this stress. Accordingly a value is chosen which leads to slip patterns which conform in *size* with those observed. The results, as regards slip on plane A, are given in *fig. 8*. The direction of the hatching indicates the orientation of the effective slip plane A. As regards plane D, of course, the same figure applies. The slip planes B and C give rise to other patterns which are displaced about 70° (the tetrahedral angle) with respect to each other, but are otherwise similar to each other; in this case only the radial stress component is of influence.

In order to be able to make some predictions regarding the pattern of the etch pits in a given cross-section we must superimpose the individual distributions obtained in this way, taking into account that only those dislocations will give rise to etch pits that lie in planes which do not make too small an angle with the plane of the cross-section. For an elliptical (111) cross-section (// to D, say) of a [110] rod only the dislocations associated with slip in the planes A, B and C will be observed. The result of the above considerations is represented in *fig. 9a* for such a (111) cross-section. This theoretical figure can now be compared with the observed pattern shown in fig. 3*a*. They agree very satisfactorily, both as regards the radial distribution of the etch-pit density (minimum in annular region roughly half-way along the radius, owing to the substantial equality of the opposing resolved components of axial and radial stresses), and as regards the azimuthal variations at the periphery (minima at an angle of about 45° with the axes of the ellipse).

Theoretical etch-pit figures for the other orientations investigated can be derived in an analogous way. An example is shown in fig. 9*b*, which should be compared with the experimental pattern in fig. 3*b*. Again, the agreement is very satisfactory.

These results thus indicate that we were justified in making the assumption that only a slight degree of plastic deformation occurs during cooling. The alternative, namely that complete plastic stress-relaxation occurs, appears on the other hand to lead

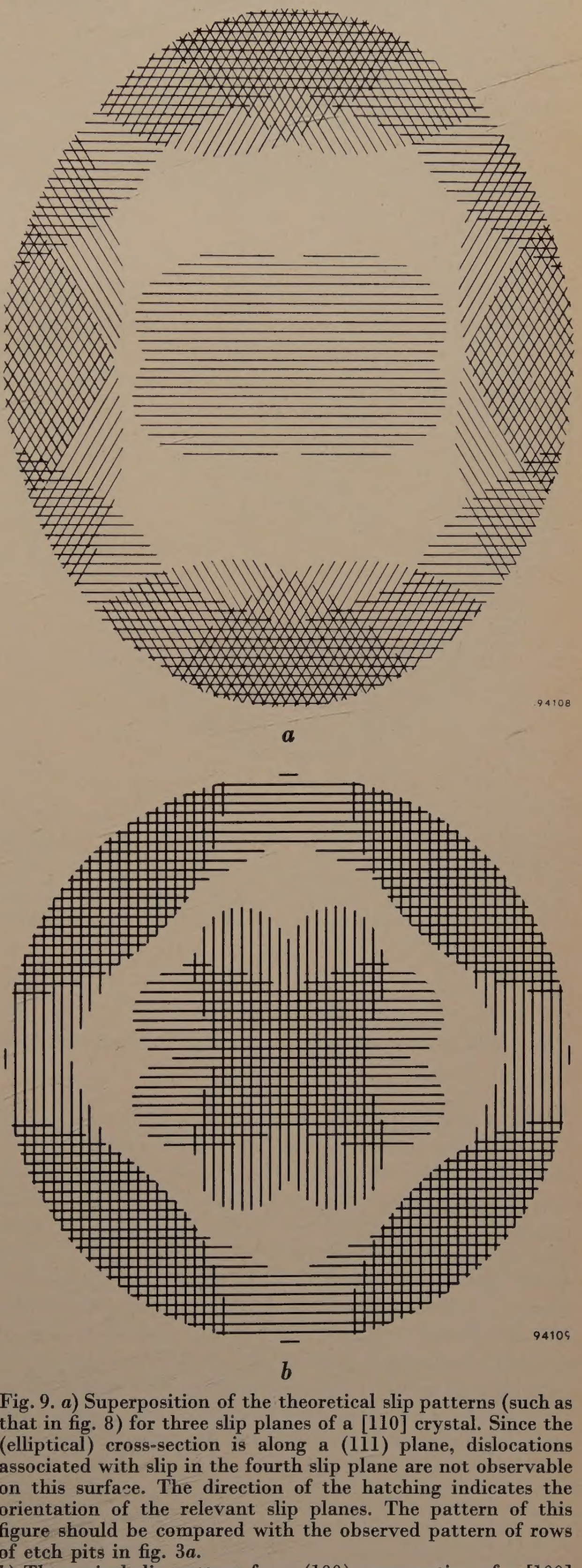

Fig. 9. *a*) Superposition of the theoretical slip patterns (such as that in fig. 8) for three slip planes of a [110] crystal. Since the (elliptical) cross-section is along a (111) plane, dislocations associated with slip in the fourth slip plane are not observable on this surface. The direction of the hatching indicates the orientation of the relevant slip planes. The pattern of this figure should be compared with the observed pattern of rows of etch pits in fig. 3*a*.
b) Theoretical slip pattern for a (100) cross-section of a [100] crystal. Compare with fig. 3*b*.

to theoretical etch-pit distributions (*fig. 10*) which differ considerably from those actually observed. (It may be noted here that a number assumptions concerning the plastic deformation of germanium are necessarily involved in the derivation of fig. 10. The assumptions seem reasonable but their validity has not actually been verified.)

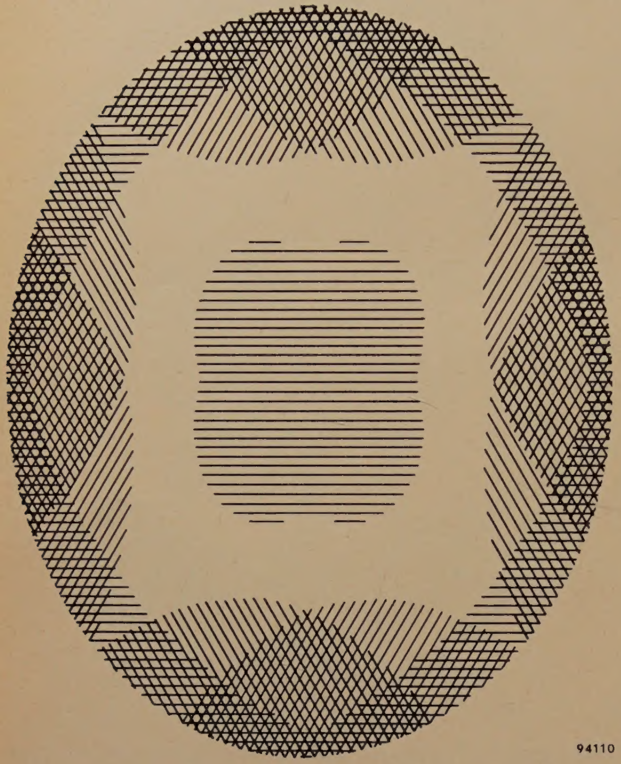

Fig. 10. Theoretical "slip figure" for the orientation in fig. 3*a* and fig. 9*a*, derived on the assumption of complete stress relaxation by plastic flow. The agreement between this figure and fig. 3*a*, is not nearly as good as between fig. 9*a* and fig. 3*a*, as appears, for example, from the shape of the central maximum and the position of the peripheral minima (the latter are almost absent in the figure above).

It may be asked why much greater plastic deformations do not occur. A possible answer might be based on the delay in plastic flow already mentioned, which characterizes the formation of new dislocations in germanium under the influence of deforming stresses. Although this delay time can no longer be measured in normal deformation tests above 600 °C, it can be shown that in the very short times elapsing during the first stages of cooling of a germanium rod (e.g. 0.1 sec. for the first 100 °C cooling) the number of dislocations that can be formed under the influence of thermal stresses does not amount to more than about 10% of the minimum number that would be necessary for a complete stress-relaxation. The cause of this delay in plastic flow is probably to be sought in the homopolar bonding forces between the atoms in the germanium lattice, which obstruct the movement of dislocations, or in an analogous influence arising from impurities, or in both.

Thermal stresses during crystal growth

From the good agreement between the observed etch-figures on quenched rods and the theoretical patterns derived above from considerations of slip, we may conclude that dislocations will also arise during the withdrawal of crystals from the melt. The perfection of the crystals will be determined by the thermal stresses present, and can thus be influenced by modifying the conditions during growth. As mentioned early in this article, a unifrom temperature gradient in the crystal will entail no thermal stresses. This state, however, can never be achieved because losses due to external radiation and, of course, the movement of the crystal, give rise to a heat flux resulting in a non-uniform temperature gradient in the crystal. The simple theory treated in the foregoing is, of course, unable to give a quantitative description of the very complicated situation during the growth of the crystal. We might, in addition, introduce an axial temperature gradient into the theory but even then we can only partially approach the actual situation. Qualitatively, however, the theory gives a good explanation of several aspects of the formation of dislocations during the withdrawal process: for example, the effect on the dislocation distribution when the crystal is rotated — a method employed for producing a crystal of good cylindrical shape.

Summary. During the pulling of germanium and silicon crystals from the melt, a process widely employed in practice, a non-uniform temperature gradient arises. As a result, thermal stresses are formed in the material which may cause plastic flow or even fracture of the material Some experiments are described concerning the influence of the rate of cooling of a germanium rod on the state of internal perfection of the material. The latter can be judged, after polishing and etching, by the number of etch pits observed under the microscope and their distribution over a cross-section of the rod. These etch pits are formed at those places where a dislocation line terminates at the face of the cross-section. The distribution and density of the dislocations depend on the degree of plastic deformation, and this in turn depends on the spatial distribution of the thermal stresses. These stresses are derived for a cylindrical rod with radial heat flux. For various crystallographic orientations of the rod, theoretical patterns of etch-pit distribution are derived which are in very good agreement with the figures observed. The theoretical figures are based on the assumption that the stresses are only partially relieved by plastic flow. This assumption, evidently justified by the good agreement found, throws an interesting light on the properties of dislocations in homopolar substances such as germanium.